Edge dynamics in quantum Hall bilayers: Exact results with disorder and parallel fields

J. D. Naud,[1] L. P. Pryadko,[2,*] and S. L. Sondhi[1]
[1]*Department of Physics, Princeton University, Princeton, New Jersey 08544*
[2]*School of Natural Sciences, Institute for Advanced Study, Olden Lane, Princeton, New Jersey 08540*
(Received 12 June 2000; published 12 February 2001)

We study edge dynamics in the presence of interlayer tunneling, parallel magnetic field, and various types of disorder for two infinite sequences of quantum Hall states in symmetric bilayers. These sequences begin with the 110 and 331 Halperin states and include their fractional descendants at lower filling factors; the former is easily realized experimentally while the latter is a candidate for the experimentally observed quantum Hall state at a total filling factor of 1/2 in bilayers. We discuss the experimentally interesting observables that involve just one chiral edge of the sample and the correlation functions needed for computing them. We present several methods for obtaining exact results in the presence of interactions and disorder that rely on the chiral character of the system. Of particular interest are our results on the 331 state, which suggest that a time-resolved measurement at the edge can be used to discriminate between the 331 and Pfaffian scenarios for the observed quantum Hall state at filling factor 1/2 in realistic double-layer systems.

DOI: 10.1103/PhysRevB.63.115301 PACS number(s): 73.43.−f, 71.10.Pm, 72.80.Ng

I. INTRODUCTION

The dynamics of the edge modes in quantum Hall systems has been a subject of great interest for some years.[1–3] Its appeal is multifold. The low-energy excitations of the ideal quantum Hall states that give rise to the plateau in the Hall resistance exist only at the edges. There is a deep connection between the structure of the bulk ground states and the ''universal content'' of the edge dynamics that is captured mathematically in a relation between $(2+1)$-dimensional Chern-Simons theories and $(1+1)$-dimensional conformal field theories.[4,5] This connection in turn implies a nontrivial charge dynamics at the edge, which is now supported by experiments.[6,7] Finally, this connection allows the logic to be turned around in deducing new quantum Hall states from an analysis of possible conformal field theories.[5,8]

In this paper we investigate the edge dynamics of two infinite sequences of quantum Hall states in statistically symmetric bilayer systems in which we supplement the universal content by the inclusion of interlayer electron tunneling, an additional magnetic field parallel to the layers and, most importantly, disorder. The chief interest of this problem is that interlayer tunneling is strongly affected by the nontrivial charge dynamics and thus serves as an ''internal probe'' of the latter. In a previous publication,[9] henceforth denoted I, we had studied the problem of the nondisordered system that gives rise to a chiral version of the sine-Gordon theory that is exactly soluble for the two infinite families of states for which interlayer tunneling is not irrelevant: these are the $mm'n$ Halperin states with $m=m'=n+1$ and $m=m'=n+2$. The second of these families was shown to exhibit a remarkable *trifurcation* of charged excitations on the edge with the appearance of two Majorana fermions with dynamically generated velocities. In this paper we consider the additional effect of disorder and a nonzero temperature on the dynamics as well as the possibilities of modifying the tunneling by means of an interlayer magnetic field or a gated transfer of charge between the layers; the latter two procedures are essentially equivalent as we will see below.

While the additional complications, especially the disorder, do not allow a complete solution in the sense of finding distributions of correlation functions in interlayer fields and at finite temperatures, the chiral character of the dynamics still allows us to make substantial progress in ways that should be of considerable interest to readers with a background in the physics of interacting, disordered systems. Consequently, we have included some amount of technical detail in the paper. In order not to lose sight of the principal physical results, especially those on the 331 state and the double-layer Pfaffian state that are experimentally testable, this introduction is followed by a summary of the ''useful content'' of the paper. Readers primarily interested in this summary may wish to stop their perusal at its end.

Before proceeding to that summary, a brief discussion of the observables and the relevant correlation functions is in order. As we will show in more detail below, we study systems that possess one edge mode per layer so their single-layer analogs are the Laughlin states at $\nu=1/m$ with m odd. In those cases a *single* edge presents three natural observables.[10] The first is the ground-state expectation value of the edge current, which can, in principle, be significant if the flux through the bulk is varied.[11] The second is the tunneling density of states, computed from the one-electron Green's function, and the last is the edge mode velocity measured in a time-resolved experiment done at the edge, which enters the retarded density-density correlation function. In reality, the first is not experimentally relevant, while the third is not remarkable when there is one mode that is unaffected by disorder or temperature. The second has been experimentally investigated[6,7] to great effect if not theoretical satisfaction; see Ref. 12 and references therein.

One of our central contentions is that the collective mode structure *is* interesting in double-layer systems, even in the minimal cases where there is only one edge mode per layer. This was already clear in the clean cases considered previously, as in the trifurcation alluded to above, and is also the case in the more involved and realistic cases studied here. Consequently, the computation of retarded density correlators central to time- and layer-resolved measurements at the edges will be a central concern. In addition we will also

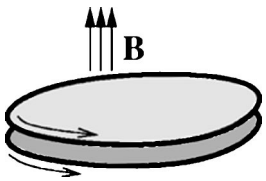

FIG. 1. The overall geometry of the bilayer quantum Hall system in a magnetic field B with edge modes in both layers propagating in the same direction.

compute one-electron Green's functions needed for tunneling measurements, but they will turn out to be essentially insensitive to the perturbations that we consider. We will not compute edge currents, although our results on partition functions in I can be easily extended to do so in clean systems, and extensions to the cases studied here are also feasible.

We should note that some of this work has technical connections to earlier work on single-layer systems[13,14] with multiple-edge modes but the details are different, and one of our sequences, inclusive of the 331 Halperin state relevant to experiments, has no analog in single layer systems.

The outline of the paper is as follows. We begin with a review of the edge theory of clean bilayer systems in the presence of uniform interlayer tunneling at the edge (Sec. II A). Next we present our results for the effects of an interlayer magnetic field (Sec. II B), disorder (Sec. II C), and a finite temperature (Sec. II D). The experimental consequences are discussed in Sec. II E, and the details of the calculations are presented in Sec. III and the appendixes.

II. SUMMARY OF RESULTS

In this section we present a summary of our results. Readers interested in the details of the calculations will find them in Sec. III, which also contains formal definitions of the parameters of the model. We begin with a review of the edge theory of clean bilayer systems. Next we consider the inclusion of a parallel magnetic field, disorder, and a finite temperature. We conclude with an experimental proposal for an edge measurement that could determine the bulk state responsible for the $\nu=1/2$ plateau observed in bilayer systems.

A. Review of clean bilayer edge theory

The system under study consists of two parallel two-dimensional electron gases (2DEG's) in a strong perpendicular magnetic field. The geometry is sketched in Fig. 1. Specifically, we are interested in the edge excitations of the Halperin states described by the mmn wave function,

$$\Psi_{m,m,n}(\{z_{i\alpha}\})=\prod_{\alpha<\beta}(z_{1\alpha}-z_{1\beta})^m(z_{2\alpha}-z_{2\beta})^m \times\prod_{\alpha,\beta}(z_{1\alpha}-z_{2\beta})^n\exp\left(-\sum_{i,\alpha}|z_{i\alpha}|^2/4\right), \tag{1}$$

where $z_{i\alpha}$ is the complex coordinate of electron α in layer i. The integer m determines the correlations within the layers and the integer n specifies the interlayer correlations. These states are incompressible and thus the gapless excitations of the system are confined to the droplet edges, which have length L and are parametrized by the coordinate x.

The edge theory contains two chiral Bose fields, a charged mode ϕ_c and a neutral mode ϕ. We denote the velocities of these modes by $v_{c,n}$, respectively. Excitations of the charged mode correspond to charge being added to the edge from the bulk, whereas excitations of the neutral mode correspond to a transfer of charge between the edges of the two layers. We restrict our discussion to states for which both edge modes move in the same direction, the ''maximally chiral'' case, by requiring $m>n$.

In I it was shown that in the presence of interlayer single-electron tunneling at the edge, the Hamiltonian of the edge theory separates into a free chiral boson Hamiltonian for the charged mode and a chiral sine-Gordon Hamiltonian (χSG) for the neutral mode. The chiral sine-Gordon Hamiltonian depends on the scaled tunneling strength, denoted λ, and the parameter $\hat{\beta}\equiv\sqrt{2(m-n)}$, which sets the period of the interaction term as well as the engineering dimension of λ [see Eq. (37)]. Since the neutral-mode Hamiltonian depends only on $m-n$, the set of all maximally chiral bilayer states can be divided into sequences labeled by the value of this difference. In particular, we will concentrate on the 110 sequence, which contains all states with $m-n=1$, and the 331 sequence, composed of states with $m-n=2$. The tunneling perturbation is relevant, in a renormalization group (RG) sense, for the 110 sequence and marginal for the 331 sequence.

The 110 and 331 sequences were solved exactly in I. In particular the single-electron Green's function

$$\mathcal{G}_{ij}(t,x)\equiv -i\langle T{:}\Psi_i(t,x){::}\Psi_j^\dagger(0,0){:}\rangle \tag{2}$$

and the two-point function of the density-fluctuation operator

$$i\mathcal{D}_{ij}(t,x)\equiv\langle T\rho_i(t,x)\rho_j(0,0)\rangle-\langle\rho_i(t,x)\rangle\langle\rho_j(0,0)\rangle, \tag{3}$$

where Ψ_i and ρ_i are the electron annihilation and charge density operators on the edge of layer i, respectively, were computed exactly at zero temperature and $L\to\infty$. We reproduce these results here, adopting a self-evident matrix notation. For the 110 sequence we have

$$\mathcal{G}(t,x)=\frac{\mathbb{1}\cos(\lambda x/v_n)+i\sigma^x\sin(\lambda x/v_n)}{[2\pi(x-v_c t+i\epsilon_t)]^{m-1/2}\sqrt{2\pi(x-v_n t+i\epsilon_t)}}, \tag{4}$$

$$-i\mathcal{D}(t,x)=\frac{1}{2(2m-1)}\frac{(\mathbb{1}+\sigma^x)}{[2\pi(x-v_c t+i\epsilon_t)]^2}+\frac{(\mathbb{1}-\sigma^x)}{2}\frac{\cos(2\lambda x/v_n)}{[2\pi(x-v_n t+i\epsilon_t)]^2}, \tag{5}$$

where $\mathbb{1}$ is the 2×2 unit matrix, σ^x is the standard Pauli matrix and $\epsilon_t \equiv \mathrm{sgn}(t)a$, where a is a short distance cutoff of the order of the magnetic length. For the 331 sequence we find

$$\mathcal{G}(t,x)=\frac{1}{[2\pi(x-v_c t+i\epsilon_t)]^{m-1}}\frac{1}{2}\left[\frac{\mathbb{1}+\sigma^x}{2\pi(x-v_1 t+i\epsilon_t)}+\frac{\mathbb{1}-\sigma^x}{2\pi(x-v_2 t+i\epsilon_t)}\right], \tag{6}$$

$$-i\mathcal{D}(t,x)=\frac{1}{4(m-1)}\frac{(\mathbb{1}+\sigma^x)}{[2\pi(x-v_c t+i\epsilon_t)]^2}+\frac{1}{4}\frac{(\mathbb{1}-\sigma^x)}{2\pi(x-v_1 t+i\epsilon_t)2\pi(x-v_2 t+i\epsilon_t)}, \tag{7}$$

where we have defined the velocities $v_{1,2}\equiv v_n \pm \lambda/\pi$. Each of these functions contains a part arising from the charged mode and a part from the neutral mode. For the single-electron Green's functions the contributions from each mode are combined multiplicatively, while for the density-density correlation function they are combined additively.

In addition to these time-ordered correlation functions, in later sections we will be interested in the corresponding retarded functions that govern physical response measurements at the edge. The density response function is

$$\mathcal{D}^R(t,x)=-\frac{\theta(t)}{2\pi}\left[\frac{(\mathbb{1}+\sigma^x)}{2(2m-1)}\delta'(x-v_c t)+\frac{(\mathbb{1}-\sigma^x)}{2}\cos(2\lambda x/v_n)\delta'(x-v_n t)\right] \tag{8}$$

for the 110 sequence and

$$\mathcal{D}^R(t,x)=-\frac{\theta(t)}{2\pi}\left[\frac{(\mathbb{1}+\sigma^x)}{4(m-1)}\delta'(x-v_c t)+\frac{(\mathbb{1}-\sigma^x)}{4(v_1-v_2)x}\{v_2\delta(x-v_2 t)-v_1\delta(x-v_1 t)\}\right] \tag{9}$$

for the 331 sequence, where the prime denotes differentiation with respect to the argument.

We see that for the 110 sequence relevant tunneling produces spatial oscillations in the correlation functions, while for the 331 sequence marginal tunneling leads to two velocities ($v_{1,2}$) in the neutral-mode sector, and hence a total of *three* velocities for the system as a whole. Note that even at zero temperature and in the absence of disorder the signal from the neutral mode in the density-density response function decays with distance because of tunneling. In the following section we shall investigate how these correlation functions are modified by various perturbations.

B. Parallel field

We first discuss the effects of an interlayer magnetic field. If we take the z axis along the normal to the layers and recall that the x axis is along the edges, we consider an additional magnetic field along the y axis: $\mathbf{B}=B\hat{\mathbf{y}}$. The edge Hamiltonian in the presence of a parallel field depends on the parameter $\Gamma \equiv v_n B d\hat{\beta}/2$, where d is the layer separation. We remark that the effect of the interplane magnetic field considered here is distinct from the simple decrease in λ caused by the reduction of the interlayer tunneling matrix element. As noted by Chalker and Sondhi, these effects can be distinguished by studying large-aspect-ratio samples.[15] The results here also apply to the case where we introduce an electric potential difference between the layers instead of an interplane magnetic field.

1. 110 sequence

For the states in the 110 sequence we find that the spectrum of the edge theory in the presence of an interlayer magnetic field can be obtained from the spectrum with zero interlayer field via the replacement

$$\lambda \mapsto \lambda' \equiv \sqrt{\lambda^2+\Gamma^2/2}; \tag{10}$$

in particular, we see that the number of velocities is unchanged. The two-point function of the density-fluctuation operator (3) is

$$-i\mathcal{D}(t,x)=\frac{1}{2(2m-1)}\frac{(\mathbb{1}+\sigma^x)}{[2\pi(x-v_c t+i\epsilon_t)]^2}+\frac{1}{2(\lambda')^2}\frac{(\mathbb{1}-\sigma^x)}{[2\pi(x-v_n t+i\epsilon_t)]^2}\left\{\frac{\Gamma^2}{2}+\lambda^2\cos\left(\frac{2\lambda' x}{v_n}\right)\right\}. \tag{11}$$

Note that in the absence of tunneling ($\lambda=0$), the correlation function is unaffected by the parallel magnetic field, i.e., it is independent of Γ, as expected. For nonzero tunneling, the addition of an interlayer magnetic field increases the frequency and decreases the amplitude of the spatial oscillations in the density-density correlation function. One can show that the effect of the parallel field on the single-electron Green's function is similar to its effect on the density two-point function; see Eq. (59).

2. 331 sequence

For the states in the 331 sequence we find that in the presence of an interlayer magnetic field the spectrum of the neutral-mode portion of the edge theory is

$$\mathcal{H}_B = \sum_k \varepsilon(k) : a_k^\dagger a_k :, \tag{12}$$

where

$$\varepsilon(k) \equiv v_n k + \mathrm{sgn}(\Gamma)\sqrt{(\lambda k/\pi)^2 + \Gamma^2},$$

where the a_k are canonical Fermi operators. Note that in the limit of vanishing parallel magnetic field, $\Gamma \to 0^+$, the energy dispersion (for $\lambda > 0$) becomes $\varepsilon(k) = (v_n + \lambda/\pi)k = v_1 k$ for $k > 0$ and $\varepsilon(k) = (v_n - \lambda/\pi)k = v_2 k$ for $k < 0$, which is the spectrum of two right-moving Majorana fermions with split velocities. (In the limit $\Gamma \to 0^-$, or for $\lambda < 0$, we get a similar dispersion with v_1 and v_2 interchanged, but this does not alter the excitation spectrum of the Hamiltonian.) For any nonzero interplane field we find that the dispersion develops some curvature, which corresponds to the two Majorana species being mixed at distances large compared with $\lambda/\pi\Gamma$. The dispersion is sketched in Fig. 2.

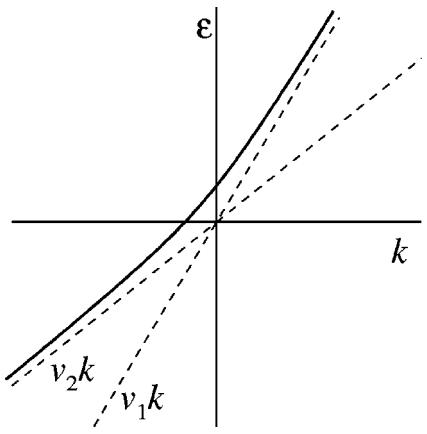

FIG. 2. The solid line is the dispersion $\varepsilon(k)$ plotted for $\Gamma > 0$. The dashed lines are $\varepsilon = v_1 k$ and $\varepsilon = v_2 k$. Note that $\varepsilon(k)$ asymptotically tends to $v_1 k$ as $k \to \infty$ and $v_2 k$ as $k \to -\infty$.

The correlation functions for the 331 sequence with a parallel field can be reduced to quadrature. If we define the quantities $\tau \equiv \mathrm{sgn}(t)(v_n X - t)$,

$$X \equiv \frac{x}{v_1 v_2}, \quad \kappa(\omega) \equiv \sqrt{v_1 v_2 \Gamma^2 + (\lambda/\pi)^2 \omega^2}, \tag{13}$$

and the function

$$P(\tau, X) \equiv \int_0^\infty \frac{d\omega}{2\pi} e^{i\omega\tau} \frac{\sin[\kappa(\omega)X]}{\kappa(\omega)}, \tag{14}$$

then the single-electron Green's function and the density-density correlation function can be expressed in terms of $P(\tau, X)$ and its derivatives. We find

$$\mathcal{G}(t,x) = \frac{-i\,\mathrm{sgn}(t)}{v_1 v_2 [2\pi(x - v_c t + i\epsilon_t)]^{m-1}} \left[\left(v_n \mathbb{1} - \frac{\lambda}{\pi}\sigma^x \right) P_X(\tau, X) + \mathrm{sgn}(t) \left(\frac{\lambda}{\pi}\mathbb{1} - v_n \sigma^x \right) \frac{\lambda}{\pi} P_\tau(\tau, X) - i v_1 v_2 \Gamma \sigma^z P(\tau, X) \right], \tag{15}$$

$$-i\mathcal{D}(t,x) = \frac{1}{4(m-1)} \frac{(\mathbb{1} + \sigma^x)}{[2\pi(x - v_c t + i\epsilon_t)]^2} - \frac{(\mathbb{1} - \sigma^x)}{4 v_1 v_2} \left[P_X^2 - \frac{\lambda^2}{\pi^2} P_\tau^2 + v_1 v_2 \Gamma^2 P^2 \right], \tag{16}$$

where the subscripts on P denote partial differentiation.

In Fig. 3 we plot the real and imaginary parts of the neutral-mode part of $\mathcal{G}_{11}$ at fixed $X = 10$ as a function of $-\tau$ for $v_n = 1$, $\Gamma = 0.5$, and $\lambda/\pi = 0.1$. The corresponding plot for the neutral mode part of $\mathcal{G}_{12}$ is given in Fig. 4. The singularities visible in these plots occur at the points $t = x/v_1$ and $t = x/v_2$, corresponding to propagation at the Majorana velocities. We see that the parallel field does not destroy the velocity-split structure of the Green's function, which is somewhat remarkable. The parallel field is a RG relevant perturbation that modifies the low-energy, long-wavelength properties of the system; see Fig. 2. Nevertheless, the singularities at v_1 and v_2 are completely unchanged, see Eq. (166) below, since they arise from integrations over all frequencies. In Appendix B we will discuss the opposite case: a RG irrelevant perturbation that does modify some features of the Green's function. At times corresponding to propagation velocities between v_1 and v_2 we find oscillatory behavior not present at $\Gamma = 0$.

C. Disorder

We now consider the effects of disorder on the bilayer system. Our primary interest is how the novel features of the correlation functions in the presence of tunneling, i.e., spatial oscillations in the 110 sequence and the splitting of the neutral-mode Majorana velocities in the 331 sequence, are modified by disorder. Note that the quantities of physical interest are the correlation functions in a typical realization of disorder, whereas the readily calculable quantities are disorder-averaged correlation functions. The typical and average quantities may have very different behavior, and we will discuss such differences at various points.

In addition to the possibility of disorder in the tunneling amplitude, λ, we consider random scalar potentials, $\xi_i(x)$,

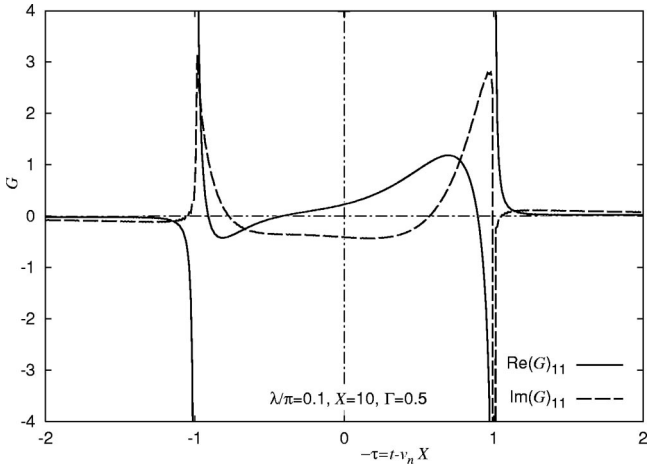

FIG. 3. The real (solid line) and imaginary (dashed line) parts of the neutral-mode factor in $\mathcal{G}_{11}$ [Eq. (74)] plotted as a function of $-\tau$ for $v_n=1$, $\lambda/\pi=0.1$, $X=10$, and $\Gamma=0.5$.

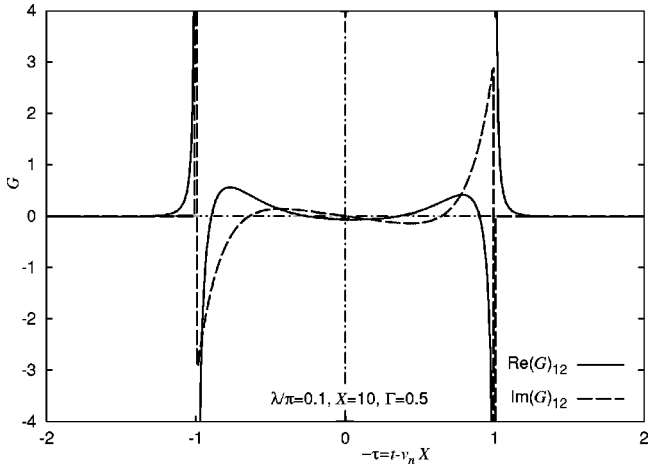

FIG. 4. The real (solid line) and imaginary (dashed line) parts of the neutral-mode factor in $\mathcal{G}_{12}$ [Eq. (74)] plotted as a function of $-\tau$ for $v_n=1$, $\lambda/\pi=0.1$, $X=10$, and $\Gamma=0.5$.

which couple to the edge charge densities in each layer. From a perturbative RG analysis we find that disorder in λ is relevant for the 110 sequence and irrelevant for the 331 sequence, while the random scalar potentials, $\xi_i(x)$, are relevant for both sequences.

1. 110 sequence

We consider a tunneling amplitude that has mean λ and variance Δ_λ and a disordered scalar potential with zero mean and variance Δ_ξ. We find that the disorder-averaged, retarded density response function is

$$\overline{\mathcal{D}^R}(t,x,x')=-\frac{\theta(t)}{2\pi}\left\{\frac{(\mathbb{1}+\sigma^x)}{2(2m-1)}\delta'(x-x'-v_c t)\quad+\frac{(\mathbb{1}-\sigma^x)}{2}\delta'(x-x'-v_n t)e^{-2|x-x'|(\Delta_\lambda+\Delta_\xi/4)/v_n^2}\right.$$
$$\left.\times\left[\cos\left(\frac{2|x-x'|\tilde{\lambda}}{v_n}\right)+\frac{\Delta_\xi}{4v_n\tilde{\lambda}}\sin\left(\frac{2|x-x'|\tilde{\lambda}}{v_n}\right)\right]\right\}, \tag{17}$$

where

$$\tilde{\lambda}\equiv\sqrt{\lambda^2-\left(\frac{\Delta_\xi}{4v_n}\right)^2}. \tag{18}$$

The disorder in the tunneling amplitude (Δ_λ) produces an exponential decay with distance in the neutral-mode part of the disorder-averaged density response function. The random scalar potential (Δ_ξ) has a similar effect, and in addition it produces a shift in the frequency of the spatial oscillations (18). Using the fact that the neutral-mode part of $\mathcal{D}$ in a given sample can be expressed in terms of products of single-particle Green's functions, whose absolute squares are long-ranged (i.e., algebraically decaying), we can conclude that in a given sample the density response function has the structure of the disorder-averaged quantity (17), without the exponential decay in space of the neutral-mode piece.

2. 331 sequence

Above we remarked that for the 331 sequence only disorder in the scalar potential terms was a nonirrelevant perturbation. We therefore consider only a disordered scalar potential with zero mean and variance Δ_ξ. We find that the disorder-averaged, retarded density response function at $T=0$ is

$$\overline{\mathcal{D}^R}(t,x,x')=-\frac{\theta(t)}{2\pi}\frac{\mathbb{1}+\sigma^x}{4(m-1)}\delta'(x-x'-v_c t)+\frac{\mathbb{1}-\sigma^x}{4}\overline{D^R}(t,x,x'), \tag{19}$$

where the neutral-mode contribution is

$$\overline{D^R}(t,x,0)=\frac{\theta(t)}{2\pi}e^{-\Delta_\xi x/v_1v_2}\left\{\frac{1}{(v_1-v_2)x}\{v_1\delta(x-v_1t)-v_2\delta(x-v_2t)\}+\frac{\Delta_\xi}{2v_1v_2}\theta(z)\mathrm{P}\left(\frac{1}{t_0-t}\right)\right.$$
$$\left.\times\left[\frac{x/v_1v_2}{\sqrt{z}}I_1\left(\frac{\Delta_\xi}{\lambda/\pi}\sqrt{z}\right)+\frac{\pi}{\lambda}I_0\left(\frac{\Delta_\xi}{\lambda/\pi}\sqrt{z}\right)\right]\right\}. \tag{20}$$

Here $z\equiv(t-x/v_1)(x/v_2-t)$, I_n are Bessel functions of imaginary argument, and $t_0\equiv(x/v_1+x/v_2)/2=v_\mathrm{n}x/v_1v_2$ is the mean arrival time.

Comparing this expression to the result for the neutral mode in a clean system, the second term in Eq. (9), we find that the δ-function peaks at the velocities v_1 and v_2 remain sharp in the presence of disorder, but their amplitudes acquire an additional exponential decay. In the disorder-averaged result, Eq. (20), there is also a signal centered around the mean arrival time t_0. If we write $\tau=t_0-t$, then in the limit of large distances $x/v_1v_2\gg1/\Delta_\xi$; for times near the mean arrival time, $(\pi/\lambda)\tau\ll x/v_1v_2$, the central signal is asymptotically

$$\overline{D^R}(t,x,0)\approx\sqrt{\frac{\Delta_\xi}{x}}\mathrm{P}\left(\frac{1}{\tau}\right)\exp\left[-\frac{\Delta_\xi v_1v_2}{2x(\lambda/\pi)^2}\tau^2\right]. \tag{21}$$

This asymptotic form is similar to a result obtained by Wen for the case of two $\nu=1$ edges with unequal velocities.[13] The reason for this similarity is that both problems are formally equivalent to a spin in a random magnetic field that undergoes diffusion on the SU(2) group manifold; see Appendix A. The term in Eq. (21) decays algebraically with distance. Therefore, while the signal in $\overline{D^R}$ at the extremal velocities ($v_{1,2}$) is exponentially suppressed by the disorder, there is an additional signal with velocity v_1v_2/v_n that only falls off algebraically.

To determine the behavior of D^R in a given realization of disorder we have adopted several approaches. First, as in our analysis of the 110 sequence, we can use the fact that D^R can be expressed in terms of single-particle Green's functions whose second moments we can evaluate. Second, we have found that $D^R(t,x,x')$ exhibits an exact antisymmetry about the point $t=t_0$ in each realization of disorder:

$$D^R(t_0+t,x,x')=-D^R(t_0-t,x,x'). \tag{22}$$

This is an interesting result because it is an exact dynamical symmetry (i.e., it is a relation between correlation functions at different times) in a system with an arbitrary potential $\xi(x)$. Finally, we have calculated the behavior of the correlation functions for two simple potentials: the case of a uniform potential $\xi(x)=\mathrm{const}$, and the case of isolated δ-function impurities $\xi(x)=\Sigma_m q_m\delta(x-y_m)$. All of these results, discussed in detail in Sec. III C, lead us to the conclusion that $D^R(t,x,x')$ in a typical configuration is given by an expression similar to Eq. (20) for $\overline{D^R}(t,x,x')$, with the principal value factor replaced by a function $f(t,x,x')$, which is a rapidly fluctuating function of time, antisymmetric about the point $t=t_0$, and whose amplitude grows as t approaches t_0. These conclusions about the behavior of D^R in a given sample have been verified by numerical simulations that are discussed in Sec. II E.

D. Finite-temperature effects

We now briefly consider the effects of a finite temperature $T=1/\beta$. For a single chiral edge mode we know that at zero temperature $\mathcal{D}^R(t,x)\propto\theta(t)\delta'(x-vt)$. A straightforward calculation shows that this form is actually temperature independent.

Recall that for the 110 sequence the retarded density-density correlation function is a sum of terms of the form $\theta(t)\delta'(x-vt)$ multiplied by a function independent of t. This can be seen for the clean system in Eq. (8) and for the disordered system in Eq. (17). We can therefore conclude that $\mathcal{D}^R$ for the 110 sequence is temperature independent even in the presence of a nonzero scalar potential.

The situation is different for the 331 sequence. While the term in $\mathcal{D}^R$ from the charged mode is temperature independent for the reasons given above, the neutral-mode term is not. At a finite temperature one finds for the neutral-mode in a clean system:

$$D^R(t,x)=-\frac{\theta(t)}{2\beta v_1v_2}\frac{1}{\sinh[\pi(v_1-v_2)x/\beta v_1v_2]}$$
$$\times[v_2\delta(x-v_2t)-v_1\delta(x-v_1t)]. \tag{23}$$

Comparing this with the zero-temperature result, the second term in Eq. (9), we find that the neutral-mode term, which decays as $1/x$ at $T=0$, decays exponentially at $T>0$.

In the presence of disorder one finds that the finite-temperature form of $\overline{D^R}$ is

$$\overline{D^R}(t,x,0)=\frac{\theta(t)}{2\pi}e^{-\Delta_\xi x/v_1v_2}\left\{\frac{(\pi/\beta v_1v_2)}{\sinh[\pi(v_1-v_2)x/\beta v_1v_2]}\{v_1\delta(x-v_1t)-v_2\delta(x-v_2t)\}+\Delta_\xi\theta(z)\mathrm{P}\left(\frac{(\pi/\beta v_1v_2)}{\sinh[2\pi(t_0-t)/\beta]}\right)\right.$$
$$\left.\times\left[\frac{x/v_1v_2}{\sqrt{z}}I_1\left(\frac{\Delta_\xi}{\lambda/\pi}\sqrt{z}\right)+\frac{\pi}{\lambda}I_0\left(\frac{\Delta_\xi}{\lambda/\pi}\sqrt{z}\right)\right]\right\}. \tag{24}$$

This result was obtained using the formalism given in Appendix A.

Comparing this with the zero-temperature result in Eq. (20) we see that the amplitudes of the δ functions at the extremal velocities acquire an additional exponential decay because of the finite temperature. However, the replacement

$$\mathrm{P}\left(\frac{1}{t_0-t}\right)\mapsto\mathrm{P}\left(\frac{(2\pi/\beta)}{\sinh[2\pi(t_0-t)/\beta]}\right) \tag{25}$$

indicates that the structure in $\overline{D^R}$ centered on the mean arrival time *sharpens* at a finite temperature.

E. Experimental ramifications

One of the primary results of the previous sections is the unusual structure of the retarded density-density correlation function for the 331 sequence. The first state in the 331 sequence, the state 331 itself, has a filling factor of 1/4 per layer, for a total filling factor of 1/2. A plateau in the Hall conductance has been experimentally observed at $\nu=1/2$ in bilayer systems.[16] Another candidate state that has been proposed to explain this plateau is the Pfaffian state.[17] Standard experimental probes of the edge states, such as the nonlinear *I-V* characteristic, cannot be used to distinguish the 331 from the Pfaffian state since both states give the same power law exponent.[18] In this section, we argue that the retarded density-density correlation function of the Pfaffian state is sufficiently different from that predicted for the 331 state such that, even in the presence of a finite temperature and disorder, a measurement of this correlation function at the edge could distinguish between these two bulk states.

For the Pfaffian edge theory we find that the retarded density response function at a finite temperature and in the presence of disorder is

$$\mathcal{D}^R_{\mathrm{Pf}}(t,x)=-\frac{1}{4\pi}\theta(t)\,\delta'(x-v_\varphi t). \tag{26}$$

We see that there is only a single velocity present.

Recall from Sec. II A, Eq. (9), that for the 331 edge there are three velocities present in the clean system at zero temperature, one for the charged mode (v_c) and two for the neutral mode ($v_{1,2}$), whose splitting is due to tunneling. The signal at the two neutral-mode velocities decays as $1/x$ at $T=0$ in the clean system. In Sec. II C we saw that a disordered scalar potential suppresses the signal at the extremal velocities by a factor that decays exponentially with distance. However, we found that there is a broad signal in the neutral mode, centered on a velocity distinct from the charged-mode velocity, which decays only algebraically. In Sec. II D we saw that a finite temperature actually sharpens the signal centered on the mean arrival time. From the results and discussion in Secs. II C and II D, we expect that for the 331 edge in a given realization of disorder, the structure of the retarded finite-temperature density-density correlation function is

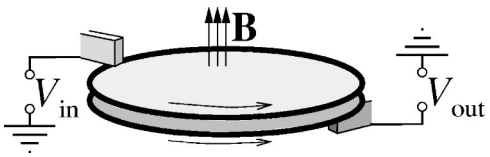

FIG. 5. The experimental geometry showing the quantum Hall bilayer in a magnetic field B with two spatially separated contacts. A density disturbance is produced at one electrode (V_{in}) and measured at the other electrode (V_{out}).

$$\mathcal{D}^R_{331}(t,x,x')\approx\theta(t)(\mathbb{1}+\sigma^x)\,\delta'(x-v_c t) + \theta(t)(\mathbb{1}-\sigma^x)\frac{f(t,x,x',\beta)}{\sqrt{l(x-x')}}\exp\left[-\frac{(t-t_0)^2}{l(x-x')}\right], \tag{27}$$

where the function $f(t,x,x',\beta)$ is the finite-temperature version of the function introduced at the end of Sec. II C, and l is a length scale set by the potential. We expect $f(t,x,x',\beta)$ to have the same properties as the zero-temperature function, and to have its support more strongly concentrated near $t=t_0$ as the temperature increases.

The experiment we propose involves creating a density disturbance at one point along the edge of the bilayer system and measuring the signal some distance downstream. The experimental geometry is sketched in Fig. 5. Basic linear response theory states that if the density disturbance is produced in layer j via an external potential $V_{\mathrm{ex}}(t,x)$ and measured in layer i, then the signal is

$$\langle\rho_i(t,x)\rangle_{\mathrm{ex}}=\int dt'dx'\mathcal{D}^R_{ij}(t-t',x,x')V_{\mathrm{ex}}(t',x'). \tag{28}$$

If the external potential is turned on at a point, i.e., $V_{\mathrm{ex}}(t',x')=\delta(x')\theta(t')$, then the measured signal is

$$\langle\rho_i(t,x)\rangle_{\mathrm{ex}}=\int_{-\infty}^{t}dt'\mathcal{D}^R_{ij}(t',x,0). \tag{29}$$

For the Pfaffian state one would see a single sharp signal; see Eq. (26). In contrast, for the 331 state, in addition to a sharp signal from the charged mode there would be a second signal from the neural mode. To illustrate the neutral-mode signal one would expect in this case we have performed numerical simulations. A typical trace, computed at zero temperature for $v_n=1$, $\lambda/\pi=0.1$, $X=10$, $\Delta_\xi=0.1$ with stepwise-constant disorder potential with $N_x=2^7$ values is shown in Fig. 6 with a solid line. As expected, it is a rapidly fluctuating function, but it exhibits an exact symmetry about the mean arrival time. This symmetry follows from the antisymmetry of D^R [Eq. (22)] and the time integration [Eq. (29)]. Although the signal is very noisy, a measurement with finite resolution (dashed line) produces a curve that does not average to zero. The amplitude of the smoothened signal is maximal at the mean arrival time as was predicted in Sec. II C. In Fig. 7 we show the result of numerically averaging over 1600 impurity configurations (solid line), as well as the analytic average (dashed line) evaluated using Eq. (20). The

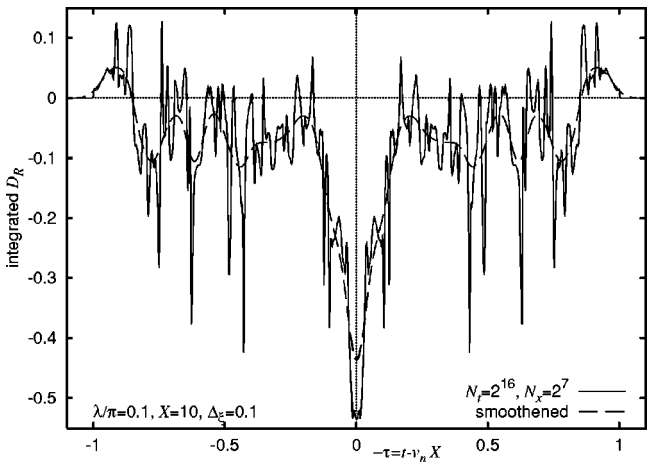

FIG. 6. The neutral-mode contribution to the integrated $\mathcal{D}_{12}^R$ [Eq. (29)] at $T=0$ for $v_n=1$, $\lambda/\pi=0.1$, $X=10$, and $\Delta_\xi=0.1$. The horizontal axis is time measured from the mean arrival time. The solid line is for a given realization of disorder, and the dashed line assumes a measurement with a finite time resolution.

two curves are in excellent agreement. The finite width of the neutral-mode signal is a novel feature of the 331 state; in the 110 sequence the neutral mode propagates with only one velocity.

In Fig. 8 we show a similar trace, but with the disorder stronger by an order of magnitude, $\Delta_\xi=1.0$. Note that the amplitude of the signal near the extremal arrival times $\tau=\pm 1$ is suppressed relative to the case with a smaller disorder strength, but the signal near the mean arrival time ($\tau=0$) is not. In Fig. 9 we show the result for $\Delta_\xi=0.1$ at a high temperature $T/\Delta_\xi=2000$. The signal in a given realization of disorder (thin solid line) is as noisy as in the zero-temperature case (Fig. 6); however, the amplitude of the smoothened signal (dashed line) is down by roughly an order of magnitude. At this high temperature the disorder-averaged result (thick solid line) is essentially zero everywhere except very close to the mean arrival time.

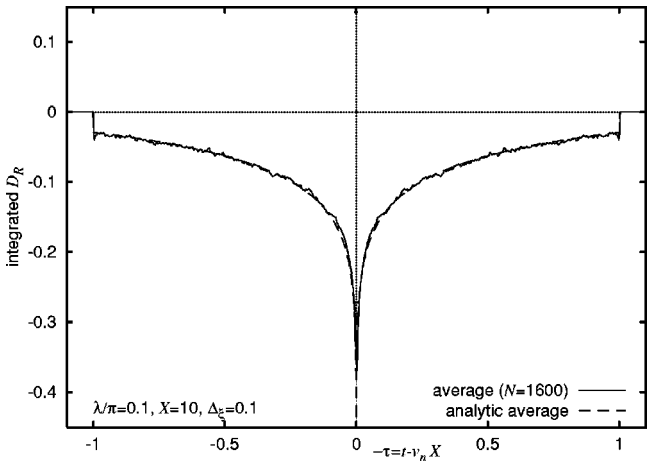

FIG. 7. The neutral-mode contribution to the integrated $\mathcal{D}_{12}^R$ [Eq. (29)] at $T=0$ for $v_n=1$, $\lambda/\pi=0.1$, $X=10$, and $\Delta_\xi=0.1$. The solid line is the numerical average over 1600 impurity configurations and the dashed line is the analytical result.

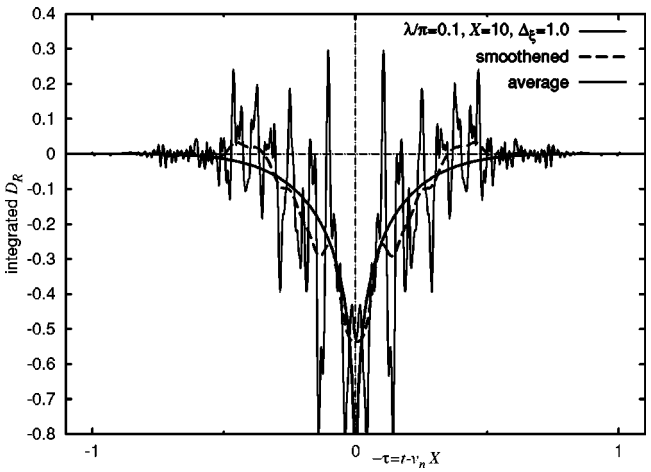

FIG. 8. The neutral-mode contribution to the integrated $\mathcal{D}_{12}^R$ [Eq. (29)] at $T=0$ for $v_n=1$, $\lambda/\pi=0.1$, $X=10$, and $\Delta_\xi=1.0$. The thin solid line is for a given realization of disorder, the dashed line assumes a measurement with a finite time resolution, and the thick solid line is the analytical average.

There are several requirements that must be met to make the measurement useful. First, one must be able to separately (or at least differentially) contact the edges of the bilayer system. If each electrode used in the measurement couples identically to both edges, one cannot hope to probe the dynamics of the neutral mode. Indeed, the sum of the elements of the matrix density-density correlation function for the 331 state [Eq. (19)] is identical in form to that of the Pfaffian state [Eq. (26)]. The relative strength of the signal from the neutral mode, compared to the charged mode, would be maximized by applying a voltage that is antisymmetric between the layers. Second, the experiment must involve a time-resolved measurement in order to distinguish signals that differ by their propagation velocities. Third, the electrodes must be close enough together so that the decay of the

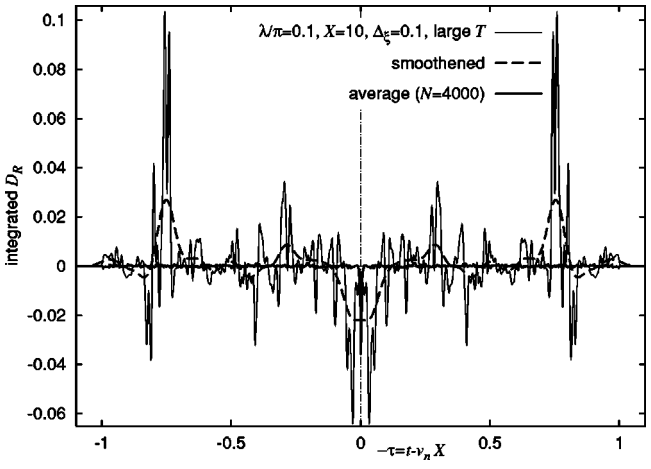

FIG. 9. The neutral-mode contribution to the integrated $\mathcal{D}_{12}^R$ [Eq. (29)] at $T/\Delta_\xi=2000$ for $v_n=1$, $\lambda/\pi=0.1$, $X=10$, and $\Delta_\xi=0.1$. The thin solid line is for a given realization of disorder, the dashed line assumes a measurement with a finite time resolution, and the thick solid line is the result of averaging over 4000 impurity configurations.

neutral-mode signal with distance does not cause it to be undetectable, but they must be far enough apart so that the charged- and neutral-mode signals are well separated in time.

We believe that the length and time scales needed in a realistic measurement would require a careful choice of fabrication techniques. To give more specific estimates, let us take the drift velocity of the charge mode to be $v_c \sim 10^7$ cm/s.[19,20] In a clean system at a finite temperature the strength of the neutral-mode signal decays exponentially with distance; see Eq. (23). The separation between the electrodes here cannot be taken to be much larger than the temperature coherence length $L_T \sim \hbar v/T$, which is 10^{-2} cm at 10 mK. Assuming the neutral-mode velocity is smaller than the charged-mode velocity by an order of magnitude, the arrival time difference between the two modes is on the order of 10 ns. In the presence of disorder, the temperature coherence length loses its importance, as one can see from the second term in Eq. (24). In this case, let us assume a mean free path of $l \sim 1/\Delta_\xi \sim 10^{-5}$ cm, and require that the electrodes need to be approximately $100l \sim 10$ μm apart for the neutral-mode signal to be detectable. The arrival time difference between the signals from the neutral and charged modes is then around 1 ns. If an experimental measurement like the one described here detected the neutral-mode signal, it would conclusively show that the $\nu = 1/2$ plateau in bilayer systems is the 331 state rather than the Pfaffian state.

III. DETAILS OF THE CALCULATIONS

In this section we present the detailed calculations of the results summarized in the previous section. We begin with a review of the clean edge theory (Sec. III A), and then discuss the addition of a parallel magnetic field (Sec. III B) and disorder (Sec. III C). Finally we discuss the Pfaffian edge (Sec. III D) and the numerical computations performed for the 331 edge (Sec. III E).

A. Edge theory of clean bilayer systems

In this section we review the edge theory of clean bilayer quantum Hall systems with interlayer electron tunneling. For a more detailed discussion see I. The edge theory corresponding to the Halperin state (1) contains two chiral Bose fields, $u_i(t,x)$ $(i=1,2)$, with compactification radii $R_i = 1$ (i.e., $u \approx u + 2\pi$), and equal-time commutation relations:

$$[u_i(t,x), u_j(t,x')] = i\pi K_{ij}\,\mathrm{sgn}(x-x'), \tag{30}$$

where K is a symmetric, integer-valued matrix that characterizes the topological properties of the edge and is completely determined by the exponents in the bulk wave function[21]

$$K = \begin{pmatrix} m & n \\ n & m \end{pmatrix}. \tag{31}$$

In terms of these fields we can write the charge density and electron creation operators as

$$\rho_i(x) = \frac{1}{2\pi} K_{ij}^{-1} \partial_x u_j(x), \quad \Psi_i^\dagger(x) = \frac{1}{L^{m/2}} e^{-iu_i(x)}, \tag{32}$$

and the Hamiltonian as

$$\mathcal{H}_0 = \int_{-L/2}^{L/2} dx \left[\frac{1}{4\pi} V_{ij} :\partial_x u_i \partial_x u_j: + \lambda_0 [:\Psi_1(x)\Psi_2^\dagger(x): + \mathrm{H.c.}] \right], \tag{33}$$

where

$$V = \begin{pmatrix} v & g \\ g & v \end{pmatrix} \tag{34}$$

is a symmetric, positive definite ($g^2 < v^2$) matrix that includes the effect of the confining potentials and interactions at the edge, and λ_0 is the interlayer electron tunneling amplitude, which we take to be real without loss of generality. The normal ordering is with respect to the oscillator modes of the bosonic fields.

The Hamiltonian and commutation relations can be simplified by the transformation:

$$\begin{pmatrix} u_1 \\ u_2 \end{pmatrix} = \frac{1}{\sqrt{2}} \begin{pmatrix} \sqrt{m+n} & -\sqrt{m-n} \\ \sqrt{m+n} & \sqrt{m-n} \end{pmatrix} \begin{pmatrix} \phi_c \\ \phi_n \end{pmatrix}, \tag{35}$$

in terms of which we have

$$[\phi_i(x), \phi_j(x')] = i\pi\delta_{ij}\,\mathrm{sgn}(x-x') \tag{36}$$

and

$$\mathcal{H}_0 = \int_{-L/2}^{L/2} dx \left[\frac{1}{4\pi} v_c :(\partial_x \phi_c)^2: + \frac{1}{4\pi} v_n :(\partial_x \phi_n)^2: + \frac{2\lambda}{(2\pi a)^{\hat{\beta}^2/2}} \cos(\hat{\beta}\phi_n) \right], \tag{37}$$

where in ϕ_i, the index i runs over the two values i=c, n, which denote the charged and neutral modes, respectively, and we have introduced the parameters $\hat{\beta} \equiv \sqrt{2(m-n)}$, $\lambda \equiv \lambda_0 L^{-n}$, the velocities $v_{c,n} = (m \pm n)(v \pm g)$, and the short distance cutoff a. The Hamiltonian separates into a free chiral boson Hamiltonian for the charged mode and a chiral sine-Gordon Hamiltonian for the neutral-mode.

For future reference we record the expression for the electron and density operators in terms of the newly introduced bosons

$$\Psi_{1,2}(x) = \frac{1}{L^{m/2}} e^{i\sqrt{(m+n)/2}\phi_c(x)} e^{\mp i\hat{\beta}\phi_n(x)/2}, \tag{38}$$

$$\rho_{1,2}(x) = \frac{1}{2\pi\sqrt{2(m+n)}} \partial_x \phi_c(x) \mp \frac{1}{2\pi\hat{\beta}} \partial_x \phi_n(x), \tag{39}$$

which follow from Eqs. (32) and (35). In the remainder of the paper we will suppress the subscript on the neutral boson, i.e., $\phi \equiv \phi_{\rm n}$.

The time-ordered correlation functions given in Sec. II A follow from Eqs. (37), (38), and (39); for details see I. To transform from the time-ordered correlation functions to the retarded response functions we note that if the time-ordered function is expressed as

$$C(t) = \theta(t)C^{>}(t) + \theta(-t)C^{<}(t), \tag{40}$$

where $\theta(t)$ is the Heaviside step function, then the corresponding retarded correlation function is

$$C^{R}(t) = \theta(t)[C^{>}(t) - C^{<}(t)]. \tag{41}$$

B. Parallel field

We consider a parallel magnetic field along the y axis: $\mathbf{B} = B\hat{\mathbf{y}}$. This corresponds to a vector potential $\mathbf{A}(z) = Bz\hat{\mathbf{x}}$, where we take the origin of the z axis midway between the layers, whose separation is d. We incorporate this parallel field into our edge theory by modifying the charge density operator via the replacement

$$\rho_i(x) \mapsto \rho_i(x) - \frac{1}{2\pi} A^x(z_i), \tag{42}$$

where $z_{1,2} = \pm d/2$. Using this along with the definition of the charge density (32), and the transformation (35) gives a Hamiltonian

$$\mathcal{H}_B \equiv \mathcal{H}_0 + \int_{-L/2}^{L/2} dx \left[\frac{\Gamma}{2\pi} \partial_x \phi + \frac{\Gamma^2}{4\pi v_{\rm n}} \right], \tag{43}$$

where $\Gamma \equiv v_{\rm n} B d\, \hat{\beta}/2$. The second term is a constant, and thus produces only an overall shift in the energy spectrum, and we will henceforth ignore it. The interlayer magnetic field couples only to the neutral mode, and therefore we will not write the terms involving the charged mode explicitly except when considering correlation functions.

As remarked in Sec. II B, the analysis here also applies to the case where we introduce an electric potential difference between the layers instead of an interplane magnetic field. A potential difference $V_{\rm e}$ between the layers adds a term $V_{\rm e}(\rho_1(x) - \rho_2(x)) \propto V_{\rm e} \partial_x \phi$ to the Hamiltonian. This is the same form as the interplane field perturbation (43). The only difference is that in the case of a potential difference between the layers the density operators are not modified as they are in the interplane magnetic field case (42). However, since $\mathcal{D}_{ij}(t,x)$ involves the density fluctuation operator, $\rho_i - \langle \rho_i \rangle$, see Eq. (3), our results below for the density-density correlation function apply for either a parallel magnetic field or an electric potential difference.

1. 110 sequence

The states in the 110 sequence correspond to $\hat{\beta}^2 = 2$. In I it is shown that at this value of $\hat{\beta}$ the radius of the neutral boson is $R_{\rm n} = 1/\sqrt{2}$ and therefore we can define a triplet of $\widehat{\rm su}(2)_1$ Kac-Moody (KM) currents

$$J^z(x) = \frac{1}{2\pi\sqrt{2}} \partial_x \phi(x),$$
$$J^{\pm}(x) = J^x \pm i J^y = \frac{1}{2\pi a} e^{\mp i\sqrt{2}\phi(x)}, \tag{44}$$

in terms of which the Hamiltonian reads

$$\mathcal{H}_B = \int_{-L/2}^{L/2} dx \left[\frac{2\pi v_{\rm n}}{3} :[\mathbf{J}(x)]^2: + \sqrt{2}\Gamma J^z(x) + 2\lambda J^x(x) \right], \tag{45}$$

where we have used the identity

$$\int_{-L/2}^{L/2} dx :[J^z(x)]^2: |\gamma\rangle = \int_{-L/2}^{L/2} dx \frac{1}{3} :[\mathbf{J}(x)]^2: |\gamma\rangle, \tag{46}$$

valid for any state $|\gamma\rangle$ in the Hilbert space. Next, we can define a new set of currents $\tilde{J}^a(x) \equiv R^{ab} J^b(x)$, which also obey an $\widehat{\rm su}(2)_1$ algebra provided $R \in {\rm SO}(3)$. In particular if we choose

$$R = \begin{pmatrix} \cos\alpha & 0 & -\sin\alpha \\ 0 & 1 & 0 \\ \sin\alpha & 0 & \cos\alpha \end{pmatrix}, \tag{47}$$

where $\sin\alpha \equiv \lambda/\sqrt{\lambda^2 + \Gamma^2/2}$, and express the rotated $\widehat{\rm su}(2)_1$ currents in terms of a new radius $R = 1/\sqrt{2}$ chiral boson, $\theta(x)$, we then have

$$\mathcal{H}_B = \int_{-L/2}^{L/2} dx \{ 2\pi v_{\rm n} :[\tilde{J}^z(x)]^2: + 2\sqrt{\lambda^2 + \Gamma^2/2}\, \tilde{J}^z(x) \} \tag{48}$$

$$= \int_{-L/2}^{L/2} dx \left[\frac{1}{4\pi} v_{\rm n} :(\partial_x \theta)^2: + \frac{1}{\pi\sqrt{2}} \sqrt{\lambda^2 + \Gamma^2/2}\, \partial_x \theta \right]. \tag{49}$$

Note that this final form of the Hamiltonian is identical to the neutral-mode Hamiltonian in the absence of a parallel magnetic field with the replacement

$$\lambda \mapsto \lambda' \equiv \sqrt{\lambda^2 + \Gamma^2/2}. \tag{50}$$

The above diagonalization of the Hamiltonian also allows us to find correlation functions. In particular, consider the two-point function of the density-fluctuation operator, $\mathcal{D}_{ij}(t,x)$ [Eq. (3)]. Using the minimal coupling prescription (42), the transformation (47), the definitions of the charge density (39), and $\widehat{\rm su}(2)_1$ currents (44), we can write

$$\rho_{1,2}(x)=\frac{1}{\sqrt{8\pi^2(2m-1)}}\partial_x\phi_c\mp\frac{1}{2\pi}\left[\frac{\Gamma}{v_n\sqrt{2}}+\frac{1}{\lambda'}\left\{\frac{\Gamma}{2}\partial_x\theta-\frac{\lambda}{a}\cos(\sqrt{2}\theta)\right\}\right]. \tag{51}$$

Using this expression for the charge density operators in terms of the fields ϕ_c and θ, along with the Hamiltonian (48), we can readily find

$$-i\mathcal{D}(t,x)=\frac{1}{2(2m-1)}\frac{(\mathbb{1}+\sigma^x)}{[2\pi(x-v_ct+i\epsilon_t)]^2}+\frac{1}{2(\lambda')^2}\frac{(\mathbb{1}-\sigma^x)}{[2\pi(x-v_nt+i\epsilon_t)]^2}\left\{\frac{\Gamma^2}{2}+\lambda^2\cos\left(\frac{2\lambda'}{v_n}x\right)\right\}. \tag{52}$$

The evaluation of the single-electron Green's function is more involved because the electron operators $[\Psi_i(x)]$ cannot be expressed in terms of the fields ϕ_c and θ. Following the method used in I, we can use the independence of the charged and neutral modes to write the Green's function, $\mathcal{G}_{ij}(t,x)$ [Eq. (2)], for all states in the 110 sequence as

$$\mathcal{G}_{ij}(t,x)=\mathcal{G}_{ij}^{(110)}(t,x)\frac{\mathcal{G}_{\phi_c}^{(m)}(t,x)}{\mathcal{G}_{\phi_c}^{(1)}(t,x)}, \tag{53}$$

where $\mathcal{G}_{ij}^{(110)}$ is the Green's function for the special case $m=1$, $n=0$ and

$$\mathcal{G}_{\phi_c}^{(m)}(t,x)\equiv\frac{1}{L^{m-1/2}}\langle e^{i\sqrt{m-1/2}\phi_c(t,x)}e^{-i\sqrt{m-1/2}\phi_c(0,0)}\rangle$$

$$=\frac{1}{[2\pi(x-v_ct+i\epsilon_t)]^{m-1/2}}. \tag{54}$$

The decomposition (53) is useful because for the *uncorrelated* integer 110 state there exists a chiral fermion description of the edge theory including tunneling and a parallel field:

$$\mathcal{H}_B^{(110)}=\int_{-L/2}^{L/2}dx:\Bigg[-iv\,\psi_i^\dagger\partial_x\psi_i+2\pi g\,\psi_1^\dagger\psi_1\psi_2^\dagger\psi_2$$

$$-\lambda(\psi_2^\dagger\psi_1+\psi_1^\dagger\psi_2)-\frac{\Gamma}{\sqrt{2}}(\psi_1^\dagger\psi_1-\psi_2^\dagger\psi_2)\Bigg]:. \tag{55}$$

Here ψ_i are the original edge electron annihilation operators given by Eq. (32) with $m=1$ and $n=0$. If we perform the following canonical transformation

$$\begin{pmatrix}\psi_1\\ \psi_2\end{pmatrix}=e^{i\varphi\sigma_y}\begin{pmatrix}\psi_+\\ \psi_-\end{pmatrix},\quad \sin(2\varphi)=-\frac{\lambda}{\lambda'}, \tag{56}$$

then the Hamiltonian (55) becomes

$$\mathcal{H}_B^{(110)}=\int_{-L/2}^{L/2}dx:[-iv(\psi_+^\dagger\partial_x\psi_++\psi_-^\dagger\partial_x\psi_-)$$

$$+2\pi g\,\psi_+^\dagger\psi_+\psi_-^\dagger\psi_--\lambda'(\psi_+^\dagger\psi_+-\psi_-^\dagger\psi_-)]:. \tag{57}$$

By transforming into boson form according to $\psi_\pm(x)=e^{i\phi_\pm(x)}/\sqrt{2\pi a}$, and defining $\theta_+\equiv(\phi_++\phi_-)/\sqrt{2}$, and $\theta_-\equiv(\phi_+-\phi_-)/\sqrt{2}-\sqrt{2}\lambda' x/v_n$, we can exactly evaluate the single-electron Green's function

$$\mathcal{G}^{(110)}(t,x)=\frac{1}{2\pi\sqrt{(x-v_ct+i\epsilon_t)(x-v_nt+i\epsilon_t)}}$$

$$\times\exp\left[i\left(\frac{\Gamma}{\sqrt{2}}\sigma^z+\lambda\sigma^x\right)\frac{x}{v_n}\right]. \tag{58}$$

Combining Eqs. (53), (54), and (58), we finally arrive at

$$\mathcal{G}(t,x)=\frac{1}{[2\pi(x-v_ct+i\epsilon_t)]^{m-1/2}\sqrt{2\pi(x-v_nt+i\epsilon_t)}}\left[\mathbb{1}\cos(\lambda' x/v_n)+\frac{i}{\lambda'}\left(\frac{\Gamma}{\sqrt{2}}\sigma^z+\lambda\sigma^x\right)\sin(\lambda' x/v_n)\right]. \tag{59}$$

2. 331 sequence

The states in the 331 sequence correspond to $\hat{\beta}^2=4$. In I it is shown that at this value of $\hat{\beta}$ we can transform the neutral boson into fermion form using

$$\frac{1}{\sqrt{2\pi a}}e^{i\phi}=\psi,\quad \frac{1}{2\pi}\partial_x\phi=:\psi^\dagger\psi:,\quad \frac{i}{2\pi a^2}e^{i2\phi}=\psi\partial_x\psi. \tag{60}$$

With these identities, the neutral-mode part of the Hamiltonian (43) becomes

$$\mathcal{H}_B = \int_{-L/2}^{L/2} dx : \Big[-i v_n \psi^\dagger \partial_x \psi - i \frac{\lambda}{2\pi} (\psi^\dagger \partial_x \psi^\dagger + \psi \partial_x \psi) + \Gamma \psi^\dagger \psi \Big] : \tag{61}$$

$$= \int_{-L/2}^{L/2} dx : \Big[-\frac{i}{2} v_1 \chi_1 \partial_x \chi_1 - \frac{i}{2} v_2 \chi_2 \partial_x \chi_2 + i\Gamma \chi_1 \chi_2 \Big] :, \tag{62}$$

where we have written the chiral Dirac fermion in terms of its Majorana components: $\psi(x) = [\chi_1(x) + i\chi_2(x)]/\sqrt{2}$, where $\chi_i^\dagger = \chi_i$, and recalled $v_{1,2} = v_n \pm \lambda/\pi$. The tunneling term splits the velocities of the two Majorana fermions and the parallel field term couples them.

The Hamiltonian is quadratic and hence readily diagonalizable. If we take antiperiodic boundary conditions for the Fermi field, $\psi(x+L) = -\psi(x)$, and expand in Fourier modes according to

$$\psi(x) = \frac{1}{\sqrt{L}} \sum_k e^{ikx} c_k, \tag{63}$$

where $k \in (2\pi/L)(\mathbb{Z} + 1/2)$, the Hamiltonian (61) becomes

$$\mathcal{H}_B = \sum_k : \Big[v_n k c_k^\dagger c_k + \Gamma c_k^\dagger c_k + \frac{\lambda k}{2\pi} (c_k^\dagger c_{-k}^\dagger - c_k c_{-k}) \Big] :$$

$$= \sum_{k>0} : (c_k^\dagger \quad c_{-k}) \begin{pmatrix} v_n k + \Gamma & \lambda k/\pi \\ \lambda k/\pi & v_n k - \Gamma \end{pmatrix} \begin{pmatrix} c_k \\ c_{-k}^\dagger \end{pmatrix} :. \tag{64}$$

Employing the Bogoliubov transformation

$$\begin{pmatrix} c_k \\ c_{-k}^\dagger \end{pmatrix} = \begin{pmatrix} \cos\alpha_k & -\sin\alpha_k \\ \sin\alpha_k & \cos\alpha_k \end{pmatrix} \begin{pmatrix} a_k \\ a_{-k}^\dagger \end{pmatrix}, \tag{65}$$

where $\alpha_{-k} = -\alpha_k$, the Hamiltonian is diagonalized via the choice

$$\tan(2\alpha_k) = \frac{\lambda k}{\pi \Gamma}, \tag{66}$$

along with the restriction $2\alpha_k \in [-\pi/2, \pi/2]$, required to produce the correct spectrum in the limit $\lambda \to 0$. This yields

$$\mathcal{H}_B = \sum_k \; [v_n k + \mathrm{sgn}(\Gamma) \sqrt{(\lambda k/\pi)^2 + \Gamma^2}] : a_k^\dagger a_k :$$

$$\equiv \sum_k \; \varepsilon(k) : a_k^\dagger a_k :. \tag{67}$$

To calculate correlation functions, we first use the transformation (65), along with the expressions for α_k [Eq. (66)] and $\psi(x)$ [Eq. (63)] to express the Fermi field in terms of the mode operators that diagonalize the Hamiltonian

$$\psi(x) = \frac{1}{\sqrt{2L}} \sum_k \frac{e^{ikx}}{[(\lambda k/\pi)^2 + \Gamma^2]^{1/4}} \Big[\sqrt{\sqrt{(\lambda k/\pi)^2 + \Gamma^2} + |\Gamma|}\; a_k - \mathrm{sgn}(\Gamma \lambda k) \sqrt{\sqrt{(\lambda k/\pi)^2 + \Gamma^2} - |\Gamma|}\; a_{-k}^\dagger \Big]. \tag{68}$$

To compute the single-electron Green's function (2) we use the transformation (35) and the fermionization prescription (60) to write the electron operators (32) as

$$: \Psi_i : = \frac{1}{(2\pi a)^{(m-1)/2}} e^{i\sqrt{m-1}\phi_c} (\delta_{i1} \psi^\dagger + \delta_{i2} \psi). \tag{69}$$

Since the charged and neutral-modes are not coupled, we find

$$\mathcal{G}(t,x) = \frac{1}{[2\pi(x - v_c t + i\epsilon_t)]^{m-1}} \mathcal{G}_\psi(t,x), \tag{70}$$

where we have defined the matrix

$$\mathcal{G}_\psi(t,x) \equiv -i \begin{pmatrix} \langle T\psi(t,x)\psi^\dagger(0,0)\rangle & \langle T\psi(t,x)\psi(0,0)\rangle \\ \langle T\psi^\dagger(t,x)\psi^\dagger(0,0)\rangle & \langle T\psi^\dagger(t,x)\psi(0,0)\rangle \end{pmatrix}. \tag{71}$$

The correlation function of the fermionized neutral mode can be reduced to quadrature. Using Eqs. (67) and (68) we obtain (in the limit $L \to \infty$)

$$\mathcal{G}_\psi(t,x) = \frac{-i}{4\pi} \begin{pmatrix} 1 + (i/t)(\partial/\partial\Gamma) & (\lambda/\pi\Gamma t)(\partial^2/\partial x \partial\Gamma) \\ (\lambda/\pi\Gamma t)(\partial^2/\partial x \partial\Gamma) & 1 - (i/t)(\partial/\partial\Gamma) \end{pmatrix} I, \tag{72}$$

where there remains the integral

$$I \equiv \int dk \{ \mathrm{sgn}(t) \cos[kx - \varepsilon(k)t] + i\, \mathrm{sgn}(k - k_F) \sin[kx - \varepsilon(k)t] \}, \tag{73}$$

and the ''Fermi momentum,'' defined by $\varepsilon(k_F)=0$, is given by $k_F=-\Gamma/\sqrt{v_1 v_2}$. To simplify the result, we first change the variable of integration to $\omega\equiv\varepsilon(k)$ for $k>k_F$ and $\omega\equiv-\varepsilon(k)$ for $k<k_F$. With these substitutions and some algebra, the matrix Green's function can be written

$$\mathcal{G}_\psi(t,x)=\frac{-i}{v_1 v_2}\mathrm{sgn}(t)\left[\left(v_n\mathbb{1}-\frac{\lambda}{\pi}\sigma^x\right)P_X(\tau,X)+\mathrm{sgn}(t)\left(\frac{\lambda}{\pi}\mathbb{1}-v_n\sigma^x\right)\frac{\lambda}{\pi}P_\tau(\tau,X)-iv_1v_2\Gamma\sigma^z P(\tau,X)\right], \tag{74}$$

where we have defined $X\equiv x/v_1v_2$, $\tau\equiv\mathrm{sgn}(t)(v_nX-t)$, and the function

$$P(\tau,X)\equiv\int_0^\infty\frac{d\omega}{2\pi}e^{i\omega\tau}\frac{\sin[\kappa(\omega)X]}{\kappa(\omega)}, \tag{75}$$

where $\kappa(\omega)\equiv\sqrt{v_1v_2\Gamma^2+(\lambda/\pi)^2\omega^2}$, and the subscripts on P in Eq. (74) denote partial differentiation. Although we have been unable to evaluate $P(\tau,X)$ explicitly, the real part of this function can be calculated in closed form. This is discussed below in Sec. III C when we consider the retarded version of $\mathcal{G}_\psi$.

Turning now to the density-density correlation function, we can use the fermionization (60) to write the density operators (39) as

$$\rho_{1,2}=\frac{1}{4\pi\sqrt{m-1}}\partial_x\phi_c\mp\frac{1}{2}:\psi^\dagger\psi:. \tag{76}$$

Since the Hamiltonian in terms of ψ [Eq. (61)] is quadratic, Wick's theorem holds for this field and the density two-point function can be expressed in terms of the single-particle Green's function. Using Eqs. (76) and (3) one finds

$$-i\mathcal{D}(t,x)=\frac{1}{4(m-1)}\frac{(\mathbb{1}+\sigma^x)}{[2\pi(x-v_ct+i\epsilon_t)]^2}+\frac{(\mathbb{1}-\sigma^x)}{4}\det\mathcal{G}_\psi(t,x). \tag{77}$$

Along with Eq. (74), this gives an expression for the density-density correlation function in terms of the single function $P(\tau,X)$ and its derivatives:

$$-i\mathcal{D}(t,x)=\frac{1}{4(m-1)}\frac{(\mathbb{1}+\sigma^x)}{[2\pi(x-v_ct+i\epsilon_t)]^2}-\frac{(\mathbb{1}-\sigma^x)}{4v_1v_2}\left[P_X^2-\frac{\lambda^2}{\pi^2}P_\tau^2+v_1v_2\Gamma^2P^2\right]. \tag{78}$$

C. Disorder

We now consider the effects of adding several types of disorder to the Hamiltonian of the bilayer system (33). We begin by considering the relevancy of various random terms within a renormalization group (RG) analysis. We then present exact results for the 110 and 331 sequences, concentrating on the retarded density response function because of its relevancy for experiments. The 110 case is solved by using an SU(2) gauge transformation to separate the Green's functions into products of clean Green's functions and terms involving only the random fields. After this step, the disordered problem is shown to be equivalent to a spin-1/2 particle in a random magnetic field and the disorder averaging is performed nonperturbatively. The solution for the 331 sequence involves an exact summation of the disorder-averaged perturbation theory, which is possible because of the chirality of the system. In Appendix A we present an alternative method for obtaining disorder-averaged correlation functions for the 331 sequence based on the spin analogy.

If we consider a general perturbation to the Hamiltonian of the form

$$\mathcal{H}_\delta=\int_{-L/2}^{L/2}dx\,\zeta(x)\mathcal{O}(x), \tag{79}$$

where $\mathcal{O}(x)$ is an operator of scaling dimension δ and $\zeta(x)$ is a Gaussian random variable with variance Δ, i.e., $\overline{\zeta(x)\zeta(x')}=\Delta\,\delta(x-x')$, where the bar denotes disorder averaging, then a lowest-order perturbative RG analysis gives[22]

$$\frac{d\Delta}{dl}=(3-2\delta)\Delta, \tag{80}$$

where the short-distance cutoff increases as l increases.

Consider first the possibility of disorder in the velocity-interaction matrix V in the Hamiltonian (33). Since the V matrix multiplies an operator of scaling dimension $\delta=2$, we see from the flow equation (80) that δ-correlated disorder is RG irrelevant. Therefore we can ignore randomness in the V matrix and interpret the values appearing in Eq. (34) as disorder-averaged mean values. Note that the V matrix must be symmetric, since it multiplies a symmetric operator in the Hamiltonian, and the positive-definiteness of V is required for the Hamiltonian to be bounded from below. However, the assumption that $V_{11}=V_{22}$ is made for technical reasons and it can be relaxed to $\overline{V_{11}}=\overline{V_{22}}$, a weaker criterion.

Next we turn to the case of disorder in the tunneling amplitude λ in the Hamiltonian (37). The scaling dimension of the tunneling operator it multiplies is $\delta=\hat{\beta}^2/2$. Using Eq. (80), we find that disorder in the tunneling amplitude is relevant for the 110 sequence (i.e., $\hat{\beta}^2=2$), and irrelevant for

the 331 sequence (i.e., $\hat{\beta}^2=4$). The former case will be discussed later in this section and the latter case in Appendix B.

Finally we consider adding random scalar potentials that couple to the edge charge densities in each layer:

$$\mathcal{H}_{\xi}=\int_{-L/2}^{L/2}dx[\xi_1(x)\rho_1(x)+\xi_2(x)\rho_2(x)] =\int_{-L/2}^{L/2}dx\left[\xi_{\mathrm{c}}(x)\frac{1}{2\pi}\partial_x\phi_{\mathrm{c}}(x)+\xi_{\mathrm{n}}(x)\frac{1}{2\pi}\partial_x\phi(x)\right], \tag{81}$$

where we have used the definition of the charge density operators (39), and

$$\xi_{\mathrm{c}}\equiv\frac{1}{\sqrt{2(m+n)}}(\xi_1+\xi_2),\quad \xi_{\mathrm{n}}\equiv\frac{1}{\hat{\beta}}(\xi_2-\xi_1). \tag{82}$$

If we assume that $\xi_{1,2}(x)$ are independent Gaussian random variables, then so are $\xi_{\mathrm{c,n}}(x)$. Since these terms involve operators of scaling dimension $\delta=1$ they are relevant perturbations for both the 110 and 331 sequences.

1. 110 sequence

In the discussion above we found that for the 110 sequence ($\hat{\beta}^2=2$), disorder both in the tunneling and in the scalar potential terms is relevant. We therefore consider the Hamiltonian

$$\mathcal{H}_D=\int_{-L/2}^{L/2}dx\left[\frac{v_{\mathrm{c}}}{4\pi}:(\partial_x\phi_{\mathrm{c}})^2:+\frac{v_{\mathrm{n}}}{4\pi}:(\partial_x\phi)^2:+\frac{1}{2\pi a}[\lambda(x)e^{i\sqrt{2}\phi(x)}+\lambda^*(x)e^{-i\sqrt{2}\phi(x)}]+\xi_{\mathrm{c}}(x)\frac{1}{2\pi}\partial_x\phi_{\mathrm{c}}(x)+\xi_{\mathrm{n}}(x)\frac{1}{2\pi}\partial_x\phi(x)\right], \tag{83}$$

where $\lambda(x)$ is a complex random tunneling amplitude. The presence of disorder breaks translation invariance and hence the current algebra method used to solve the clean problem in Sec. III B is inapplicable because the transformation $\tilde{J}^a(x)=R^{ab}J^b(x)$ must be a global rotation to map between sets of KM generators. However, an alternative approach to the problem developed in I is useful in the disordered case. We add to the Hamiltonian (83) an auxiliary free chiral boson ($\hat{\phi}$) with a velocity equal to the velocity of ϕ:

$$\mathcal{H}_D\mapsto\mathcal{H}_D+\int_{-L/2}^{L/2}dx\frac{1}{4\pi}v_{\mathrm{n}}:(\partial_x\hat{\phi})^2:, \tag{84}$$

perform the canonical transformation

$$\begin{pmatrix}\hat{\phi}\\ \phi\end{pmatrix}=\frac{1}{\sqrt{2}}\begin{pmatrix}1 & 1\\ 1 & -1\end{pmatrix}\begin{pmatrix}\theta_1\\ \theta_2\end{pmatrix}, \tag{85}$$

and then transform to fermion form according to

$$\psi_i(x)=\frac{1}{\sqrt{2\pi a}}e^{i\theta_i(x)}. \tag{86}$$

The details required to make this mapping rigorous (i.e., compactification radii, topological charges, Klein factors) are discussed in I. The result of this procedure is a quadratic Hamiltonian

$$\mathcal{H}_D=\int_{-L/2}^{L/2}dx\left[\frac{1}{4\pi}v_{\mathrm{c}}:(\partial_x\phi_{\mathrm{c}})^2:+\xi_{\mathrm{c}}(x)\frac{1}{2\pi}\partial_x\phi_{\mathrm{c}}(x) +:[-iv_{\mathrm{n}}\Psi^{\dagger}\partial_x\Psi+v_{\mathrm{n}}B^a(x)\Psi^{\dagger}\sigma^a\Psi]:\right], \tag{87}$$

where we have defined

$$\Psi(x)\equiv\begin{pmatrix}\psi_1(x)\\ \psi_2(x)\end{pmatrix},$$

$$\mathbf{B}(x)=\frac{1}{v_{\mathrm{n}}}(-\mathrm{Re}[\lambda(x)],-\mathrm{Im}[\lambda(x)],\xi_{\mathrm{n}}(x)/\sqrt{2}), \tag{88}$$

and the index a runs over x,y,z. The fermionic part of this Hamiltonian describes a pseudo-spin-1/2 fermion coupled to a random SU(2) gauge field.

We now perform a change of variables that absorbs the disordered terms into the definitions of the field operators. For the charged mode we define

$$\eta(x)=\phi_{\mathrm{c}}(x)+\frac{1}{v_{\mathrm{c}}}\int^{x}dy\ \xi_{\mathrm{c}}(y), \tag{89}$$

and for the neutral mode we use an SU(2) gauge transformation

$$\Psi(x)=S(x)\tilde{\Psi}(x), \tag{90}$$

where $S(x)\in\mathrm{SU}(2)$ is a solution of the matrix differential equation

$$\frac{dS(x)}{dx}=-iB^a(x)\sigma^aS(x). \tag{91}$$

With these definitions, the Hamiltonian (87) becomes

$$\mathcal{H}_D=\int_{-L/2}^{L/2}dx\left[\frac{1}{4\pi}v_{\mathrm{c}}:(\partial_x\eta)^2:-\frac{1}{4\pi v_{\mathrm{c}}}\xi_{\mathrm{c}}^2-iv_{\mathrm{n}}:\tilde{\Psi}^{\dagger}\partial_x\tilde{\Psi}:\right]. \tag{92}$$

Since the second term only involves the disordered scalar potential, it does not affect correlation functions and will henceforth be neglected. Note that in going from Hamiltonian (87) to Hamiltonian (92) we have used a gauge trans-

formation on a chiral Fermi field (90) without accounting for the chiral anomaly. This is valid because the gauge field is a quenched random variable; in this case the anomaly associated with the chiral gauge transformation (90) cancels in the average.

Our primary goal is to understand the behavior of the density-density correlation function in a given sample, i.e., for a given realization of disorder. We begin by expressing the density operators (39) in terms of the fields η and Ψ, with the help of Eqs. (85), (86), and (89):

$$\rho_{1,2}(x)=\frac{1}{2\pi\sqrt{2(2m-1)}}\left(\partial_x\eta(x)-\frac{1}{v_c}\xi_c(x)\right) \mp\frac{1}{2}:\Psi^\dagger(x)\sigma^z\Psi(x):. \tag{93}$$

Using this expression in the definition of the density two-point function (3) we have

$$-i\mathcal{D}(t,x,x')=\frac{1}{2(2m-1)}\frac{(\mathbb{1}+\sigma^x)}{[2\pi(x-x'-v_c t+i\epsilon_t)]^2} -\frac{(\mathbb{1}-\sigma^x)}{4}\mathrm{tr}[\sigma^z G(t,x,x')\sigma^z G(-t,x',x)], \tag{94}$$

where we have used the single-particle matrix Green's function

$$G_{ij}(t,x,x')=-i\langle T\psi_i(t,x)\psi_j^\dagger(0,x')\rangle. \tag{95}$$

We have explicitly included two spatial arguments in these correlation functions because of the lack of translation invariance in a given realization of disorder. Note that although the charged mode, ϕ_c, is coupled in Eq. (81) to a disorder potential, ξ_c, the charged-mode part of the above correlation function (94) is identical to the result in the absence of disorder. This result is true for every realization of disorder and is essentially equivalent to the loop-cancellation theorem, which states that for linearly dispersing fermions $[\varepsilon(k)\propto k]$ in $1+1$ dimensions the connected n-point function of the density operator vanishes identically for $n>2$.[23]

To determine the effect of disorder on the neutral mode we first note that the differential equation (91) has a solution in terms of a coordinate-ordered exponential

$$S(x)=T_y\exp\left(-i\int^x dy\,B^a(y)\sigma^a\right), \tag{96}$$

where T_y is the y-ordering operator. Since the matrix $S(x)$ can be taken outside quantum expectation values, we can express the Green's function of the Ψ field (95) in terms of the Green's function of the (free) $\tilde{\Psi}$ field and thus write

$$G_{ij}(t,x,x')=\frac{1}{2\pi(x-x'-v_n t+i\epsilon_t)}U_{ij}(x,x'), \tag{97}$$

where

$$U(x,x')\equiv S(x)S^\dagger(x')=T_y\exp\left(-i\int_{x'}^x dy\,B^a(y)\sigma^a\right) \tag{98}$$

is a unitary matrix. Using Eq. (97) we find that the neutral-mode part of the density-density correlation function is proportional to

$$-\mathrm{tr}[\sigma^z G(t,x,x')\sigma^z G(-t,x',x)] =\frac{1}{[2\pi(x-x'-v_n t+i\epsilon_t)]^2}\mathrm{tr}[\sigma^z U(x,x')\sigma^z U^\dagger(x,x')], \tag{99}$$

where we have used the property $U^\dagger(x,x')=U(x',x)$, which follows from the definition (98). In Eq. (99) we have written a correlation function in the disordered system as the product of the corresponding function in the clean system and a factor that depends only on the random potential.

If we interpret the coordinate y appearing in the definition of U as a fictitious time, then the matrix $U(x,x')$ is exactly the time evolution operator between times x and x' for a zero-dimensional system with time-dependent Hamiltonian $B^a(y)\sigma^a$. This is the Hamiltonian for a spin-1/2 object in a random magnetic field $B^a(y)$. The quantity appearing in the trace in Eq. (99) can then be interpreted as the $\langle S_z(x)S_z(x')\rangle$ correlation function for this spin.

To understand the behavior of the density-density correlation function in a given sample we will first calculate its disorder average, which involves averaging the quantity appearing on the right hand side (r.h.s.) of Eq. (99). Toward this end, consider the following vector quantity:

$$F^a(x;x')=\mathrm{tr}[U^\dagger(x,x')\sigma^a U(x,x')\sigma^z]. \tag{100}$$

By differentiating with respect to x we find that this is a solution of the differential equation

$$\frac{dF^a(x;x')}{dx}=M^{ab}(x)F^b(x;x'), \tag{101}$$

where $M^{ab}(x)\equiv-2\epsilon^{abc}B^c(x)$, subject to the boundary condition $F^a(x';x')=\mathrm{tr}(\sigma^a\sigma^z)=2\delta^{az}$. The solution of this differential equation can also be written as

$$F^a(x;x')=\left[T_y\exp\left(\int_{x'}^x dy\,M(y)\right)\right]^{ab}F^b(x';x'). \tag{102}$$

We have expressed the quantity we desire, $F^z(x;x')$, in terms of a single coordinate-ordered matrix exponential, whose disorder average we now show can be readily evaluated.

We assume the tunneling amplitude and scalar potential are δ-correlated Gaussian random variables and denote the mean and variance of $B^a(x)$ by μ^a and Δ^a, respectively. Since the exponential appearing in Eq. (102) is ordered in y, and the elements of $M(y)$ are independently distributed for each y, we can consider breaking up the interval $[x',x]$ into N intervals of length $\epsilon=|x-x'|/N$ and then taking the limit $N\to\infty$. Therefore we can write

$$\overline{T_y \exp\left(\int_{x'}^{x} dy\, M(y)\right)} = \lim_{N\to\infty}\left[\int d\mathbf{B}\, P(\mathbf{B}) e^{\mathrm{sgn}(x-x')\epsilon M}\right]^N, \tag{103}$$

where the probability distribution is

$$P(\mathbf{B})d\mathbf{B} = \sqrt{\frac{\epsilon^3}{(2\pi)^3\Delta^x\Delta^y\Delta^z}} \times \exp\left[-\frac{1}{2}\sum_{a=1}^{3}\frac{\epsilon}{\Delta^a}(B^a-\mu^a)^2\right]d\mathbf{B}. \tag{104}$$

Expanding the $e^{\mathrm{sgn}(x-x')\epsilon M}$ factor in Eq. (103) and performing the integration gives

$$\overline{T_y \exp\left(\int_{x'}^{x} dy\, M(y)\right)} = \lim_{N\to\infty}\left[1-\frac{2|x-x'|}{N}W+O\left(\frac{1}{N^2}\right)\right]^N = \exp(-2|x-x'|W), \tag{105}$$

where

$$W \equiv \begin{pmatrix} \Delta^y+\Delta^z & 0 & 0 \\ 0 & \Delta^z+\Delta^x & 0 \\ 0 & 0 & \Delta^x+\Delta^y \end{pmatrix} + \mathrm{sgn}(x-x')\begin{pmatrix} 0 & \mu^z & -\mu^y \\ -\mu^z & 0 & \mu^x \\ \mu^y & -\mu^x & 0 \end{pmatrix}. \tag{106}$$

From Eqs. (100), (102), and (105), we finally arrive at

$$\overline{\mathrm{tr}[U^\dagger(x,x')\sigma^z U(x,x')\sigma^z]} = 2[e^{-2|x-x'|W}]^{zz}. \tag{107}$$

While it is in principle possible to evaluate the exponential of W for arbitrary μ^a and Δ^a, for simplicity we shall restrict ourselves to the case of a real tunneling amplitude. If the tunneling amplitude has mean λ and variance Δ_λ, and the disordered scalar potential has mean zero and variance Δ_ξ, then from the definition of $\mathbf{B}(x)$ [Eq. (88)] we have

$$\mu^x = -\frac{\lambda}{v_n}, \quad \mu^y = 0, \quad \mu^z = 0,$$
$$\Delta^x = \frac{\Delta_\lambda}{v_n^2}, \quad \Delta^y = 0, \quad \Delta^z = \frac{\Delta_\xi}{2v_n^2}. \tag{108}$$

In this case the x sector of the matrix (106) is separated,

$$W = \left[\frac{\Delta_\xi}{2v_n^2}\right] \oplus \left[\mathbb{1}\frac{\Delta_\lambda+\Delta_\xi/4}{v_n^2} + \sigma^z\frac{\Delta_\xi}{4v_n^2} - i\sigma^y\,\mathrm{sgn}(x-x')\frac{\lambda}{v_n}\right], \tag{109}$$

and from Eqs. (94), (99), and (107) we find

$$-i\overline{\mathcal{D}}(t,x,x') = \frac{1}{2(2m-1)}\frac{(\mathbb{1}+\sigma^x)}{[2\pi(x-x'-v_c t+i\epsilon_t)]^2} + \frac{1}{2}\frac{(\mathbb{1}-\sigma^x)}{[2\pi(x-x'-v_n t+i\epsilon_t)]^2}\exp\left(-\frac{2|x-x'|}{v_n^2}(\Delta_\lambda+\Delta_\xi/4)\right) \times\left[\cos\left(\frac{2|x-x'|\tilde{\lambda}}{v_n}\right)+\frac{\Delta_\xi}{4v_n\tilde{\lambda}}\sin\left(\frac{2|x-x'|\tilde{\lambda}}{v_n}\right)\right], \tag{110}$$

where

$$\tilde{\lambda} \equiv \sqrt{\lambda^2-\left(\frac{\Delta_\xi}{4v_n}\right)^2}. \tag{111}$$

Transforming to the corresponding retarded function using Eqs. (40) and (41) we arrive at Eq. (17).

The question remains as to what the behavior of $\mathcal{D}(t,x,x')$ is in a given sample. Instead of attempting to evaluate higher moments of this correlation function, we shall exploit the fact that it can be expressed in terms of the single-particle Green's function, whose second moment we will compute. Writing out the trace in Eq. (94) explicitly we find

$$\mathrm{tr}[\sigma^z G(t,x,x')\sigma^z G(-t,x',x)] = G_{11}(t,x,x')G_{11}(-t,x',x) - G_{12}(t,x,x')G_{21}(-t,x',x) - G_{21}(t,x,x')G_{12}(-t,x',x) + G_{22}(t,x,x')G_{22}(-t,x',x). \tag{112}$$

From Eq. (97) and the result

$$\overline{U(x,x')} = \exp\left(-\frac{|x-x'|}{2v_n^2}(\Delta_\lambda + \Delta_\xi/2)\right)\left[\mathbb{1}\cos\left(\frac{\lambda}{v_n}(x-x')\right) + i\sigma^x \sin\left(\frac{\lambda}{v_n}(x-x')\right)\right], \tag{113}$$

which can be obtained via the same procedure used to evaluate the average in Eq. (103), we find the disorder-averaged single-particle Green's functions are also exponentially decaying in space:

$$\overline{G}_{11}(t,x,x') = \overline{G}_{22}(t,x,x') = \frac{e^{-|x-x'|(\Delta_\lambda+\Delta_\xi/2)/2v_n^2}}{2\pi(x-x'-v_n t + i\epsilon_t)} \times \cos\left(\frac{\lambda}{v_n}(x-x')\right), \tag{114}$$

$$\overline{G}_{12}(t,x,x') = \overline{G}_{21}(t,x,x') = i\frac{e^{-|x-x'|(\Delta_\lambda+\Delta_\xi/2)/2v_n^2}}{2\pi(x-x'-v_n t + i\epsilon_t)} \sin\left(\frac{\lambda}{v_n}(x-x')\right). \tag{115}$$

To investigate whether this exponential decay is an artifact of the disorder averaging (i.e., it arises from averaging over random phases), or whether we expect it to hold in a given realization of disorder, we compute $\overline{|G_{ij}(t,x,x')|^2}$, which is clearly insensitive to phase fluctuations. From Eq. (97) we see that

$$\overline{|G_{ij}(t,x,x')|^2} = \frac{1}{|2\pi(x-x'-v_n t + i\epsilon_t)|^2}\,\overline{U_{ij}(x,x')U_{ji}^\dagger(x,x')}. \tag{116}$$

By the unitarity of $U(x,x')$ we have

$$\overline{U_{11}U_{11}^\dagger} + \overline{U_{12}U_{21}^\dagger} = 1, \tag{117}$$

where we have suppressed the spatial arguments. Using the explicit form of U that follows from Eqs. (98), (88), and $\mathrm{Im}[\lambda(x)]=0$, one may show $\sigma^y U^T \sigma^y = U^\dagger$, which implies

$$\overline{U_{11}U_{11}^\dagger} = \overline{U_{22}U_{22}^\dagger}, \quad \overline{U_{12}U_{21}^\dagger} = \overline{U_{21}U_{12}^\dagger}. \tag{118}$$

Finally, from Eq. (107) we have

$$\overline{U_{11}U_{11}^\dagger} - \overline{U_{21}U_{12}^\dagger} - \overline{U_{12}U_{21}^\dagger} + \overline{U_{22}U_{22}^\dagger} = 2[e^{-2|x-x'|W}]^{zz}. \tag{119}$$

Equations (117)–(119) are four equations in four unknown quantities that can be solved to yield

$$\overline{U_{11}U_{11}^\dagger} = \overline{U_{22}U_{22}^\dagger} = \frac{1}{2}(1+[e^{-2|x-x'|W}]^{zz}),$$

$$\overline{U_{12}U_{21}^\dagger} = \overline{U_{21}U_{12}^\dagger} = \frac{1}{2}(1-[e^{-2|x-x'|W}]^{zz}). \tag{120}$$

This result, combined with Eq. (116), gives the disorder-averaged absolute magnitudes of the elements of the single-particle Green's function

$$\overline{|G_{ij}(t,x,x')|^2} = \frac{1}{2|2\pi(x-x'-v_n t + i\epsilon_t)|^2}\left\{ 1 + (-1)^{i+j}\exp\left(-\frac{2|x-x'|}{v_n^2}(\Delta_\lambda + \Delta_\xi/4)\right)\left[\cos\left(\frac{2|x-x'|\tilde{\lambda}}{v_n}\right) + \frac{\Delta_\xi}{4v_n\tilde{\lambda}}\sin\left(\frac{2|x-x'|\tilde{\lambda}}{v_n}\right)\right]\right\}. \tag{121}$$

The structure of this result is interesting. Each $\overline{|G_{ij}|^2}$ is the sum of two terms, one of which is identical to the square of the free [i.e., $\lambda(x)=\xi_n(x)=0$] Green's function, and the other of which has spatial oscillations at the shifted frequency and an exponential decay in space from the disorder. The fact that $\overline{|G_{ij}|^2}$ has a long-ranged part (i.e., a term that decays algebraically rather than exponentially) indicates that in a given sample G_{ij} is not exponentially damped, and thus from Eq. (112) we can conclude that the neutral-mode portion of the density-density correlation function is also long-ranged for a given realization of disorder. We therefore expect that in a given sample the density two-point function has the structure of the disorder-averaged quantity (110), without the exponential decay in space of the neutral-mode piece. As a function of $\Delta x \equiv x - x'$ we expect two peaks at the points $\Delta x = v_{c,n} t$, with the second peak modulated in space at a frequency that varies with the local scalar potential [see Eq. (111)].

2. 331 sequence

In the analysis at the beginning of this section we determined that for the 331 sequence ($\hat{\beta}^2=4$), only disorder in the scalar potential terms was a nonirrelevant perturbation. We therefore consider the Hamiltonian

$$\mathcal{H}_D = \int_{-L/2}^{L/2} dx \left[\frac{1}{4\pi} v_c :(\partial_x \phi_c)^2: + \frac{1}{4\pi} v_n :(\partial_x \phi)^2: + \frac{\lambda}{2\pi a}(e^{i2\phi(x)} + e^{-i2\phi(x)}) + \xi_c(x)\frac{1}{2\pi}\partial_x \phi_c(x) + \xi_n(x)\frac{1}{2\pi}\partial_x \phi(x)\right], \tag{122}$$

which, with the help of the fermionization (60) for the neutral boson and the transformation (89) for the charged boson, can be written

$$\mathcal{H}_D = \int_{-L/2}^{L/2} dx : \left[\frac{1}{4\pi} v_c (\partial_x \eta)^2 - \frac{i}{2} v_1 \chi_1 \partial_x \chi_1 - \frac{i}{2} v_2 \chi_2 \partial_x \chi_2 + i \xi_n(x) \chi_1 \chi_2 \right] :, \tag{123}$$

where we have dropped the constant ξ_c^2 term. The charged-mode portion of this Hamiltonian is identical to that of Eq. (92) for the 110 sequence, and hence all results pertaining to the charged mode can be imported from the previous discussion. The Hamiltonian is now quadratic; however, the lack of translation invariance prevents us from employing the method used in Sec. III B, where we essentially solved the special case in which $\xi_c(x)$ is independent of x. In addition we cannot absorb the disorder into the definition of the field operators via a gauge transformation as we did for the 110 sequence, because the Majorana fields are real and therefore neutral. However, we can still separate the disorder and quantum expectation values by explicitly constructing solutions to the Heisenberg equations of motion. This procedure involves some technical subtleties not present in the 110 solution, and is discussed in detail in Appendix A. In this section we use a different approach; we find the disorder-averaged correlation functions of the above Hamiltonian by an *exact* summation of the disorder-averaged perturbation theory.

The chirality of the fermions in the neutral-mode part of the Hamiltonian allows a great simplification in the structure of the diagrammatic perturbation theory in powers of the disorder potential $\xi_n(x)$. This was first noted by Chalker and Sondhi in the context of a single-particle description of the edge.[15] Consider the matrix Green's function of the Majorana fields for the free case, i.e., $\xi_n(x)=0$:

$$g_{ij}^{(0)}(t,x,x') = -i\langle T \chi_i(t,x) \chi_j(0,x') \rangle = \delta_{ij} \frac{1}{2\pi(x-x'-v_j t + i\epsilon_t)}. \tag{124}$$

Fourier transforming with respect to time gives

$$g_{ij}^{(0)}(\omega,x,x') = \delta_{ij} \int dt\, e^{i\omega t} \frac{1}{2\pi(x-x'-v_j t + i\epsilon_t)} = \delta_{ij} \frac{i}{v_j} e^{i\omega(x-x')/v_j} [\theta(-\omega)\theta(x'-x) - \theta(\omega)\theta(x-x')]. \tag{125}$$

To obtain this result note that the integrand has a pole in the complex t plane at $t=(x-x')/v_j + O(\epsilon)$. Therefore for $x-x'>0$, $\mathrm{Re}\, t>0$ at the pole and hence the pole lies in the upper half-plane while for $x-x'<0$, $\mathrm{Re}\, t<0$ at the pole and it is therefore in the lower half-plane. We find that for positive frequencies ($\omega>0$) the function vanishes for $x-x'<0$, while for negative frequencies ($\omega<0$) it vanishes for $x-x'>0$.

Next consider the single-particle Majorana Green's function with the disorder potential present in Eq. (123). Working perturbatively in powers of $\xi_n(x)$, we have

$$g_{11}(\omega,x,x') = \sum_{n=0}^{\infty} \int dy_1 \cdots dy_{2n} g_{11}^{(0)}(\omega,x,y_1) \xi_n(y_1) \times g_{22}^{(0)}(\omega,y_1,y_2) \xi_n(y_2) \cdots g_{11}^{(0)}(\omega,y_{2n},x'), \tag{126}$$

$$g_{12}(\omega,x,x') = i \sum_{n=0}^{\infty} \int dy_1 \cdots dy_{2n+1} g_{11}^{(0)}(\omega,x,y_1) \times \xi_n(y_1) \cdots g_{22}^{(0)}(\omega,y_{2n+1},x'),$$

with similar expressions for the remaining components. Each time the particle scatters off the impurity potential its velocity changes from v_1 to v_2 or vice versa. When we perform a disorder average of the above equations, we must tie together insertions of $\xi_n(x)$ in all possible ways for each term in the sum. We first observe that because the scalar potential is time-independent, ω is conserved and hence it has the same sign in every propagator. This, along with the chirality of $g^{(0)}(\omega,x,x')$ evident in Eq. (125), implies that any disorder-averaged diagram in which impurity lines cross vanishes identically. Therefore, for each term in the sum in Eq. (126) there is a single nonzero disorder-averaged diagram, i.e., the one in which successive insertions of ξ_n are pairwise contracted. The resulting series can be summed to give

$$\bar{g}_{ij}(\omega,x,x') = \delta_{ij} \frac{i}{v_j} e^{i\omega(x-x')/v_j} e^{-\Delta_\xi |x-x'|/2v_1v_2} \times [\theta(-\omega)\theta(x'-x) - \theta(\omega)\theta(x-x')]. \tag{127}$$

We see that the disorder-averaged Green's function retains the chiral structure of the free Green's function. While the exponential decay of the function involves the geometric mean of the two Majorana velocities, $\sqrt{v_1 v_2}$, the frequency dependence only contains $v_{1(2)}$ for $\bar{g}_{11(22)}$. This is a direct consequence of the fact that all terms with crossed impurity lines vanish when we perform a disorder average of the chiral Green's function. Therefore, for the averaged single-particle Green's function, if the particle begins propagating with velocity v_1, it never propagates with velocity v_2, and

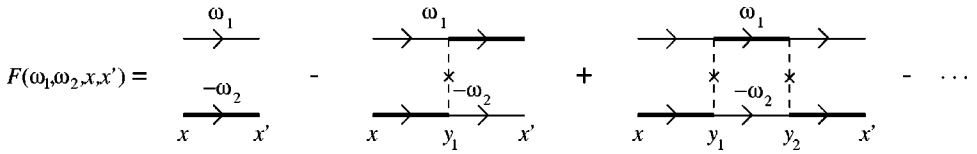

FIG. 10. Ladder sum for the neutral-mode density-density correlation function. The thin solid lines represent $\bar{g}_{11}$, the thick solid lines represent $\bar{g}_{22}$, and the dashed lines represent the disorder potential and carry a factor of Δ_ξ.

the other velocity enters only through the density of states when scattering off the potential. Transforming back to the time domain we find

$$\bar{g}_{ij}(t,x,x') = \delta_{ij} \frac{e^{-\Delta_\xi |x-x'|/2v_1v_2}}{2\pi(x-x'-v_j t + i\epsilon_t)}. \tag{128}$$

From the relation between the Dirac and Majorana fields, $\psi = (\chi_1 + i\chi_2)/\sqrt{2}$, we find that the Green's function of the neutral-mode fermion, $\mathcal{G}_\psi$ [Eq. (71)], can be obtained from g via a unitary transformation

$$\mathcal{G}_\psi(t,x,x') = O g(t,x,x') O^\dagger, \quad O \equiv \frac{1}{\sqrt{2}} \begin{pmatrix} 1 & i \\ 1 & -i \end{pmatrix}. \tag{129}$$

Thus from Eqs. (70), (127), and (129) we find, after Fourier transforming, that the single-electron Green's function for the 331 sequence in the presence of disorder is

$$\bar{\mathcal{G}}(t,x,0) \equiv \frac{1}{[2\pi(x-v_c t + i\epsilon_t)]^{m-1}} \frac{1}{2} \left[\frac{\mathbb{1} + \sigma^x}{2\pi(x - v_1 t + i\epsilon_t)} + \frac{\mathbb{1} - \sigma^x}{2\pi(x - v_2 t + i\epsilon_t)} \right] e^{-\Delta_\xi |x|/2v_1v_2}. \tag{130}$$

We see that for the single-electron Green's function the velocity split of the neutral mode remains in the presence of disorder, but the function acquires an exponential decay with distance.

We next consider the calculation of the density-density correlation function. As a first step toward understanding the behavior of this correlation function in a given sample, we will calculate its disorder average. We can use the transformation (89) and the expression for the Fermi density operator in terms of the Majorana fields, $:\psi^\dagger\psi: = :i\chi_1\chi_2:$, to write the density operators (76) as

$$\rho_{1,2} = \frac{1}{4\pi\sqrt{m-1}} \left(\partial_x \eta - \frac{1}{v_c} \xi_c \right) \mp \frac{i}{2} :\chi_1\chi_2:, \tag{131}$$

from which we find

$$-i\mathcal{D}(t,x,x') = \frac{1}{4(m-1)} \frac{(\mathbb{1} + \sigma^x)}{[2\pi(x-x'-v_c t + i\epsilon_t)]^2} - i\frac{(\mathbb{1} - \sigma^x)}{4} D(t,x,x'), \tag{132}$$

where we have denoted the neutral-mode contribution by

$$-iD(t,x,x') \equiv \langle T : \chi_1(t,x)\chi_2(t,x) :: \chi_1(0,x')\chi_2(0,x') : \rangle. \tag{133}$$

To evaluate D, we first Fourier transform with respect to time in order to exploit the chirality in the mixed frequency-space domain. Computing the expectation value in Eq. (133) using Wick's theorem and taking the disorder average then gives

$$-i\bar{D}(\omega,x,x') = -i\int dt\, e^{i\omega t} \bar{D}(t,x,x') \equiv \int \frac{d\omega'}{4\pi} F\left(\frac{\omega'+\omega}{2}, \frac{\omega'-\omega}{2}, x, x' \right), \tag{134}$$

where we have defined

$$F(\omega_1,\omega_2,x,x') = \overline{g_{11}(\omega_1,x,x') g_{22}(-\omega_2,x,x')} - \overline{g_{12}(\omega_1,x,x') g_{21}(-\omega_2,x,x')}. \tag{135}$$

If one uses Eq. (126) to write the single-particle Green's functions in the above expression in terms of the free Green's function, $g^{(0)}_{ij}$, and the disorder potential, ξ_n, one finds upon disorder averaging that the chirality of Eq. (125) implies that all nonvanishing diagrams are of the form of ladder diagrams with the legs of the ladder constructed out of the disorder-averaged propagators $\bar{g}_{ij}$.

The legs of the ladder are given by

$$h(\omega_1,\omega_2,k) \equiv \int dx\, e^{-ikx} \bar{g}_{11}(\omega_1,x,0) \bar{g}_{22}(-\omega_2,x,0) = \frac{i}{v_1v_2} \left[\frac{\theta(\omega_1)\theta(-\omega_2)}{k - \omega_1/v_1 + \omega_2/v_2 - i\Delta_\xi/v_1v_2} - \frac{\theta(-\omega_1)\theta(\omega_2)}{k - \omega_1/v_1 + \omega_2/v_2 + i\Delta_\xi/v_1v_2} \right], \tag{136}$$

which was evaluated with the help of Eq. (127) for $\bar{g}_{ij}$. The segments of the ladder shown in Fig. 10 alternate between $h(\omega_1,\omega_2,k)$ and $h(-\omega_2,-\omega_1,k)$. Performing the ladder sum gives

$$F(\omega_1,\omega_2,x,x')=\int\frac{dk}{2\pi}e^{ik(x-x')}\left[\frac{h(\omega_1,\omega_2,k)-\Delta_\xi h(\omega_1,\omega_2,k)h(-\omega_2,-\omega_1,k)}{1-\Delta_\xi^2 h(\omega_1,\omega_2,k)h(-\omega_2,-\omega_1,k)}\right]. \tag{137}$$

Using the result for $h(\omega_1,\omega_2,k)$ in this expression for $F(\omega_1,\omega_2,x,x')$ gives, after some algebra,

$$F(\omega_1,\omega_2,x,x')=\frac{i}{v_1v_2}\int\frac{dk}{2\pi}e^{ik(x-x')}\left[\theta(\omega_1)\theta(-\omega_2)\frac{k-w(\Delta_\xi)}{[k-z_+(\Delta_\xi)][k-z_-(\Delta_\xi)]}\right.$$
$$\left.-\theta(-\omega_1)\theta(\omega_2)\frac{k-w(-\Delta_\xi)}{[k-z_+(-\Delta_\xi)][k-z_-(-\Delta_\xi)]}\right], \tag{138}$$

where we have defined the parameters

$$w(\Delta_\xi)\equiv\omega_1/v_2-\omega_2/v_1+2i\Delta_\xi/v_1v_2, \tag{139}$$

$$z_\pm(\Delta_\xi)\equiv\frac{1}{v_1v_2}\left[\frac{v_1+v_2}{2}(\omega_1-\omega_2)+i\Delta_\xi\pm i\sqrt{\Delta_\xi^2-\frac{(v_1-v_2)^2}{4}(\omega_1+\omega_2)^2}\right]. \tag{140}$$

From the expression for $z_\pm(\Delta_\xi)$ we see that in the first term in Eq. (138) both poles are in the upper half-plane while in the second term both poles are in the lower half-plane. Performing the k integration by the residue theorem and using the resulting expression for F in Eq. (134) gives

$$-i\overline{D}(\omega,x,x')=\frac{1}{v_1v_2}[\theta(-\omega)\theta(x'-x)-\theta(\omega)\theta(x-x')]e^{iv_n\omega X-\Delta_\xi|X|}\int_{-\omega}^{\omega}\frac{d\omega'}{4\pi}\left[\cosh[\Lambda(\omega')X]\right.$$
$$\left.+\frac{\Delta_\xi}{\Lambda(\omega')}\sinh[\Lambda(\omega')|X|]\right], \tag{141}$$

where we have used the rescaled coordinate $X=(x-x')/v_1v_2$, and defined

$$\Lambda(\omega)\equiv\sqrt{\Delta_\xi^2-\frac{1}{4}(v_1-v_2)^2\omega^2}=\sqrt{\Delta_\xi^2-\frac{\lambda^2}{\pi^2}\omega^2}. \tag{142}$$

The experimentally measurable quantity is the retarded density-density correlation function. Since Eq. (141) is not in the time domain, we cannot use Eqs. (40) and (41) to obtain $\overline{D^R}(t,x,x')$ directly. However, in ω-k space we have the relations

$$\mathrm{Re}\,\overline{D^R}(\omega,k)=\mathrm{Re}\,\overline{D}(\omega,k),$$
$$\mathrm{Im}\,\overline{D^R}(\omega,k)=\mathrm{sgn}(\omega)\mathrm{Im}\,\overline{D}(\omega,k), \tag{143}$$

which in turn yield

$$\overline{D^R}(\omega,x)=\theta(\omega)\overline{D}(\omega,x)+\theta(-\omega)[\overline{D}(\omega,-x)]^*, \tag{144}$$

where the asterisk denotes complex conjugation. Using Eqs. (141) and (144) and Fourier transforming back to the time domain we find

$$\overline{D^R}(t,x,x')=\frac{\theta(x-x')}{2\pi}e^{-\Delta_\xi X}\mathrm{P}\left(\frac{1}{v_nX-t}\right)\int_{-\infty}^{\infty}\frac{d\omega}{2\pi}\,e^{i\omega(v_nX-t)}\left[\cosh[\Lambda(\omega)X]+\frac{\Delta_\xi}{\Lambda(\omega)}\sinh[\Lambda(\omega)X]\right], \tag{145}$$

where P denotes the principal value. The remaining integral is computed in Appendix C, and from Eqs. (C7) and (C8) we find

$$\overline{D^R}(t,x,0)=\frac{\theta(t)}{2\pi}e^{-\Delta_\xi x/v_1v_2}\left\{\frac{1}{(v_1-v_2)x}\{v_1\delta(x-v_1t)-v_2\delta(x-v_2t)\}+\frac{\Delta_\xi}{2v_1v_2}\theta(z)\mathrm{P}\left(\frac{1}{v_n x/v_1v_2-t}\right)\left[\frac{x/v_1v_2}{\sqrt{z}}I_1\left(\frac{\Delta_\xi}{\lambda/\pi}\sqrt{z}\right)+\frac{\pi}{\lambda}I_0\left(\frac{\Delta_\xi}{\lambda/\pi}\sqrt{z}\right)\right]\right\}, \tag{146}$$

where $z\equiv(t-x/v_1)(x/v_2-t)$, and I_n are Bessel functions of imaginary argument. Note that as expected this function is real. This result can also be found using the formalism in Appendix A.

We have computed $\overline{D^R}$, but what we are really interested in is the behavior of D^R in a given realization of disorder. A surprising feature of $\overline{D^R}$ is that it has a (principal value) singularity at the mean arrival time $t_0=v_n x/v_1v_2$. An immediate question is whether this singularity is present in each sample, and if not, how does it arise in the average.

To investigate the behavior of D^R in a given realization of disorder we have adopted several approaches. First, as in our analysis of the 110 sequence, we use the fact that D^R can be expressed in terms of single-particle Green's functions, whose second moments we evaluate. Second, we show that in a given sample $D^R(t,x)$ exhibits an exact symmetry about the point $t=t_0$. Finally we shall consider the behavior of the correlation functions in some simple model potentials.

The relation between the time-ordered correlation functions D and g_{ij} follows from the definition (133):

$$D(t,x,x')=i\det g(t,x,x'). \tag{147}$$

Using Eq. (40), we then conclude from the above equation that $D^>=i\det g^>$ and $D^<=i\det g^<$. Thus from Eq. (41) we have

$$D^R(t,x,x')=i\theta(t)[\det g^>(t,x,x')-\det g^<(t,x,x')]. \tag{148}$$

If we define the advanced correlation functions $g^A=\theta(-t)(g^<-g^>)$, then one can show $g^<=g-g^R$ and $g^>=g-g^A$, which when substituted into Eq. (148) give

$$D^R=i\theta(t)[(g_{11}g^R_{22}-g_{12}g^R_{21})+(g^R_{11}g_{22}-g^R_{12}g_{21})-(g^R_{11}g^R_{22}-g^R_{12}g^R_{21})]. \tag{149}$$

We see that the retarded density-density correlation function in a given sample can be expressed in terms of the time-ordered and retarded single-particle Green's functions.

We have already evaluated the average time-ordered single-particle Green's function; see Eq. (128). Using Eqs. (40) and (41) we find for the corresponding retarded function:

$$\overline{g^R_{ij}}(t,x,x')=-i\delta_{ij}\theta(t)\delta(x-x'-v_it)e^{-\Delta_\xi(x-x')/2v_1v_2}. \tag{150}$$

Next consider the absolute squares of the single-particle Green's functions. The disorder average of $g_{ij}(t,x,x')g^*_{ij}(t',x,x')$ can be evaluated by the same diagrammatic procedure used to obtain the average density-density correlation function. The disorder average of $g^R_{ij}(t,x,x')g^{R*}_{ij}(t',x,x')$ can be readily computed using the formalism presented in Appendix A.

Omitting the details of these calculations we find

$$\overline{g_{ij}(t,x,0)g^*_{ij}(t',x,0)}=\frac{1}{2\pi}\frac{e^{-\Delta_\xi|X|}}{\epsilon+i\Delta t}\int_{-\infty}^{\infty}\frac{d\omega}{2\pi}e^{i\omega(v_nX-\bar{t})-(\epsilon+i\Delta t)|\omega|/2}\left[\frac{\delta_{ij}}{v_j^2}\cosh[\Lambda(\omega)X]+\left(\frac{\sigma^z_{ij}(-i\omega\lambda/\pi)+\sigma^x_{ij}\Delta_\xi}{v_iv_j\Lambda(\omega)}\right)\times\sinh[\Lambda(\omega)X]\right], \tag{151}$$

where $\bar{t}\equiv(t+t')/2$ is the average time, $\Delta t\equiv t-t'$ is the time difference, and $\epsilon>0$ is an infinitesimal regulator. For the retarded functions we find

$$\overline{g^R_{11}(t,x,0)g^{R*}_{11}(t',x,0)}=\frac{\theta(t)}{v_1^2}\delta(\Delta t)e^{-\Delta_\xi|X|}\left[\delta(x/v_1-t)+\frac{\pi\Delta_\xi}{2\lambda}\theta(z)I_1\left(\frac{\Delta_\xi}{\lambda/\pi}\sqrt{z}\right)\sqrt{\frac{x/v_2-t}{t-x/v_1}}\right], \tag{152}$$

$$\overline{g^R_{12}(t,x,0)g^{R*}_{12}(t',x,0)}=\frac{\theta(t)}{v_1v_2}\delta(\Delta t)e^{-\Delta_\xi|X|}\frac{\pi\Delta_\xi}{2\lambda}\theta(z)I_0\left(\frac{\Delta_\xi}{\lambda/\pi}\sqrt{z}\right),$$

where we have again used $z=(t-x/v_1)(x/v_2-t)$. Note $\overline{g^R_{21}g^{R*}_{21}}=\overline{g^R_{12}g^{R*}_{12}}$, and $\overline{g^R_{22}g^{R*}_{22}}$ can be obtained from $\overline{g^R_{11}g^{R*}_{11}}$ by interchanging v_1 and v_2.

One should first observe the dependence of these quantities on the time difference $\Delta t=t-t'$. In the time-ordered case (151) the dependence is approximately $1/\Delta t$, while in the retarded case (152) it is $\delta(\Delta t)$. This suggests that in a given configuration both g and g^R are rapidly varying functions of time. The remaining integral in the time-ordered case (151) can be evaluated for the special case of equal times $\Delta t=0$, see Eqs. (C7), (C8), and (C9). One finds that $\overline{|g_{ij}(t,x,0)|^2}$ is the same as $\overline{|g^R_{ij}(t,x,0)|^2}$, provided one makes the replacement $\theta(t)\delta(0)\mapsto 1/2\pi\epsilon$. Comparing Eqs. (146) and (152) we see that the structure of the equal-time expressions, $\overline{|g_{ij}(t,x,0)|^2}$ and $\overline{|g^R_{ij}(t,x,0)|^2}$, is similar to the result for $\overline{D^R}(t,x,0)$, up to an infinite prefactor. In particular, the diagonal elements of $\overline{|g|^2}$ and $\overline{|g^R|^2}$ have δ functions with exponentially decaying amplitudes, and all elements have a term that decays algebraically at large x.

In comparing the expressions for $\overline{D^R}$ (146) and $\overline{|g^R|^2}$ [Eq. (152)], one obvious difference is the presence of the factor $\mathrm{P}[1/(t_0-t)]$ in the density-density correlation function. One consequence of this factor is that it makes $\overline{D^R}(t,x,0)$ at fixed x an odd function about $t=t_0$. We shall now demonstrate that this antisymmetry is present in each realization of disorder, not just in the averaged quantity.

The derivation of this antisymmetry relies on some of the results derived in Appendix A that allow us to express the Green's function for the disordered 331 sequence in terms of a coordinate-ordered exponential. We begin with an expression for the time-ordered, single-particle matrix Green's function in the presence of an arbitrary scalar potential $\xi(x)$, [Eq. (A16)],

$$\mathcal{G}_\psi(t,x,x')=\int\frac{d\omega}{2\pi i}e^{-i\omega t}[\theta(t)n(-\omega)-\theta(-t)n(\omega)]Q^{-1/2}S(x,x';\omega)Q^{-1/2}, \tag{153}$$

where $n(\omega)\equiv[\exp(\beta\omega)+1]^{-1}$ is the usual Fermi distribution function (with β the inverse temperature), and from Eqs. (A5) and (A10), $Q=v_n\mathbb{1}+(\lambda/\pi)\sigma^x$ and

$$S(x,x';\omega)=T_y\exp\left(i\int_{x'}^{x}dy\left[\omega Q^{-1}-\frac{\xi(y)}{\sqrt{v_1v_2}}\sigma^z\right]\right). \tag{154}$$

Equation (153) is analogous to Eq. (97) for the 110 sequence. Both equations express the Green's function in terms of a coordinate-ordered exponential. The expression for the 331 sequence is more complicated because the term in Eq. (154) describing propagation in the absence of disorder, ωQ^{-1}, does not commute with the random field term, $\xi(y)\sigma^z$.

Since $Q^{-1}=(1/v_1v_2)[v_n\mathbb{1}-(\lambda/\pi)\sigma^x]$, we can factor out an overall phase from $S(x,x';\omega)$:

$$\begin{aligned}S(x,x';\omega)&=e^{i\omega v_n(x-x')/v_1v_2}T_y\\&\quad\times\exp\left(-i\int_{x'}^{x}dy\left[\frac{\omega\lambda}{\pi v_1v_2}\sigma^x+\frac{\xi(y)}{\sqrt{v_1v_2}}\sigma^z\right]\right)\\&\equiv e^{i\omega t_0}s(x,x';\omega).\end{aligned} \tag{155}$$

Using this result and Eq. (129) to transform G_ψ to g, we find

$$g(t,x,x')=[Q^{-1/2}O]^\dagger\int\frac{d\omega}{2\pi i}e^{i\omega(t_0-t)}[\theta(t)n(-\omega)-\theta(-t)n(\omega)]s(x,x';\omega)[Q^{-1/2}O]. \tag{156}$$

From this equation we find

$$g^*(t_0+t,x,x')=-[Q^{-1/2}O]^T\int\frac{d\omega}{2\pi i}e^{i\omega t}[\theta(t_0+t)n(-\omega)-\theta(-t_0-t)n(\omega)]s^*(x,x';\omega)[Q^{-1/2}O]^*. \tag{157}$$

From the form of the matrix s [Eq. (155)], one can show

$$s^*(x,x';\omega)=\sigma^y s(x,x';\omega)\sigma^y. \tag{158}$$

Combining this with the fact that for $|t|<|t_0|$,

$$\begin{aligned}&\theta(t_0+t)n(-\omega)-\theta(-t_0-t)n(\omega)\\&\quad=\theta(t_0-t)n(-\omega)-\theta(-t_0+t)n(\omega),\end{aligned} \tag{159}$$

implies that Eq. (157) can be rewritten

$$\begin{aligned}g^*(t_0+t,x,x')&=-[Q^{-1/2}O]^T\sigma^y\int\frac{d\omega}{2\pi i}e^{i\omega t}[\theta(t_0-t)n(-\omega)-\theta(-t_0+t)n(\omega)]s(x,x';\omega)\sigma^y[Q^{-1/2}O]^*\\&=-[Q^{-1/2}O]^T\sigma^y([Q^{-1/2}O]^\dagger)^{-1}g(t_0-t,x,x')[Q^{-1/2}O]^{-1}\sigma^y[Q^{-1/2}O]^*.\end{aligned} \tag{160}$$

Therefore, if we define the matrix

$$C\equiv[Q^{-1/2}O]^T\sigma^y([Q^{-1/2}O]^\dagger)^{-1}=\begin{pmatrix}0 & -\sqrt{v_2/v_1}\\ \sqrt{v_1/v_2} & 0\end{pmatrix}, \tag{161}$$

we have the final result that

$$g(t_0+t,x,x')=-Cg^*(t_0-t,x,x')C^T,\quad\text{for }|t|<|t_0|. \tag{162}$$

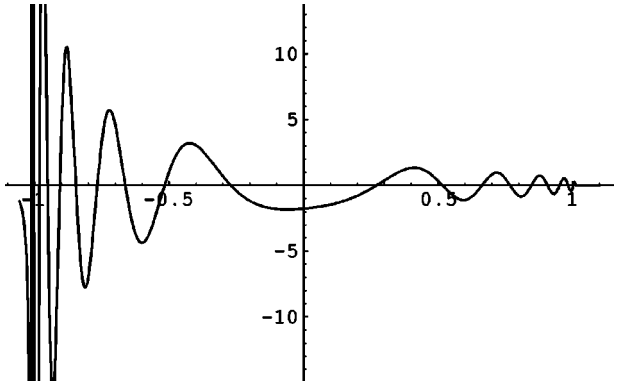

FIG. 11. The imaginary part of g^R_{11} plotted for $v_n=1$, $x=10$, $\lambda/\pi=0.1$, and $\Gamma=3$. The horizontal axis is time measured from the mean arrival time.

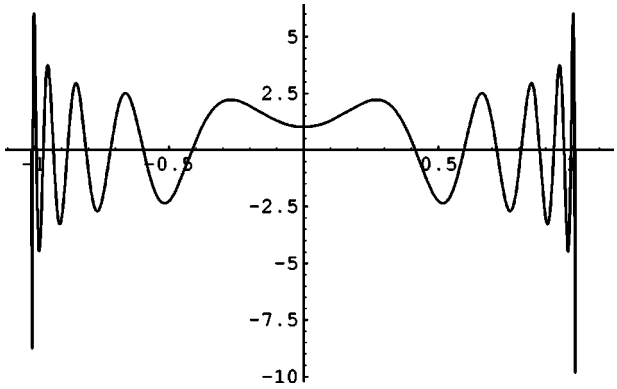

FIG. 12. The imaginary part of g^R_{12} plotted for $v_n=1$, $x=10$, $\lambda/\pi=0.1$, and $\Gamma=3$. The horizontal axis is time measured from the mean arrival time.

One can show by an analogous derivation that the corresponding retarded function, $g^R(t,x,x')$, obeys exactly the same relation.

Using the relation between D and g [Eq. (147)] and the fact that $\det C=1$, Eq. (162) implies for $|t|<|t_0|$

$$\mathrm{Re}\, D(t_0+t,x,x')=-\mathrm{Re}\, D(t_0-t,x,x'),$$

$$\mathrm{Im}\, D(t_0+t,x,x')=\mathrm{Im}\, D(t_0-t,x,x'). \tag{163}$$

Similarly, using the expression for D^R in terms of g and g^R [Eq. (149)], Eq. (162) and the corresponding relation for g^R gives

$$D^R(t_0+t,x,x')=-D^R(t_0-t,x,x'), \tag{164}$$

where we can drop the restriction $|t|<t_0$ since outside this interval D^R is identically zero from Eq. (146). We have found that the retarded density-density correlation function in a given sample is antisymmetric about the mean arrival time, indicating that the point $t=t_0$ is special, independent of $\xi_n(x)$. This result is true at any temperature. If we include disorder in the velocity so that v_n is a function of x, the symmetry (164) would be absent and the principal value singularity in $\overline{D^R}$ would be rounded out; cf. Appendix B.

Next we consider the behavior of correlation functions for some simple potentials $\xi_n(x)$. We first consider the case of a uniform potential. As we remarked in Sec. II B, the correlation functions in the presence of a parallel magnetic field can be reinterpreted as those in the presence of a uniform scalar potential difference between the layers $\xi_n(x)=\Gamma$. Using Eqs. (40) and (41) to go from the result in Sec. III B for the time-ordered single-particle Green's function, $\mathcal{G}_\psi$ [Eq. (74)], to the corresponding retarded function, and Eq. (129) to transform this to the Majorana basis, we find

$$g^R(t,x)=-\frac{2i\theta(t)}{v_1v_2}\left[\left(v_n\mathbb{1}-\frac{\lambda}{\pi}\sigma^z\right)\mathrm{Re}\, P_X(\tau,X)+\left(\frac{\lambda}{\pi}\mathbb{1}-v_n\sigma^z\right)\frac{\lambda}{\pi}\mathrm{Re}\, P_\tau(\tau,X)+iv_1v_2\Gamma\sigma^y\,\mathrm{Re}\, P(\tau,X)\right]. \tag{165}$$

The quantity $\mathrm{Re}\, P(\tau,X)$ and its derivatives are evaluated in Appendix C, and from Eqs. (C10), (C11), and (C12) we find

$$\begin{aligned} g^R_{11}(t,x)&=-i\theta(t)\left[\delta(x-v_1t)-\frac{\pi\Gamma}{2\lambda}\theta(z)J_1\left(\frac{\Gamma}{\lambda/\pi}\sqrt{v_1v_2z}\right)\sqrt{\frac{x-v_2t}{v_1t-x}}\right],\\ g^R_{12}(t,x)&=-i\theta(t)\frac{\pi\Gamma}{2\lambda}\theta(z)J_0\left(\frac{\Gamma}{\lambda/\pi}\sqrt{v_1v_2z}\right), \end{aligned} \tag{166}$$

where the J_n are standard Bessel functions. Note $g^R_{21}=-g^R_{12}$ and g^R_{22} can be obtained from g^R_{11} by interchanging v_1 and v_2. These functions are plotted in Figs. 11 and 12.

We see that the δ functions present in the diagonal elements of g^R in the case of zero potential [Eq. (150) evaluated at $\Delta_\xi=0$] remain in the case of a uniform potential. In addition to these δ functions we find oscillatory terms in all elements of $g^R(t,x)$ considered as functions of t at fixed x. Since the quantity $z=(t-x/v_1)(x/v_2-t)$ is maximal at $t=t_0$, we see that the frequency of the oscillations in g^R_{ij} is minimal at the mean arrival time and increases as we approach the extremal arrival times. This feature is evident in Figs. 11 and 12.

Finally, we consider the case of a scalar potential made up of isolated impurities located at the points $\{y_m\}$ with strengths $\{q_m\}$, i.e., we take the potential to be

$$\xi_n(x)=\sum_m q_m\delta(x-y_m). \tag{167}$$

Note that the white-noise potential used in the previous calculations can be approached by the form given in Eq. (167) if we take the number of impurities to infinity and the q_m to be random variables. Using Eq. (126), one can compute g for this potential by an exact summation of the perturbation expansion. Once again, it is the chirality of $g^{(0)}$ that makes the calculation tractable.

If there are N impurities between x and x', then the nonvanishing terms in the perturbation expansion of g_{ij} are in one-to-one correspondence with the set of all N-tuples of nonnegative integers. For example, if $x'<y_1<y_2<\cdots<y_N<x$, then for $t>0$ the nonvanishing terms correspond to propagation from x' to y_1 followed by scattering n_1 times off impurity q_1, followed by propagation from y_1 to y_2 and scattering n_2 times off impurity q_2, etc., where n_m are nonnegative integers. If n_m is even then the velocity of the particle is unchanged by the scattering (i.e., the internal lines on either side of the impurity are either both $g_{11}^{(0)}$ or both $g_{22}^{(0)}$), while if n_m is odd then the velocity of the particle is changed by the scattering (i.e., the internal lines on either side of the impurity are $g_{11}^{(0)}$ and $g_{22}^{(0)}$). Therefore, from the parity of each element n_m of the N-tuple we know which internal propagators are $g_{11}^{(0)}$ and which are $g_{22}^{(0)}$, and we can define a corresponding arrival time T. This arrival time is given by $T=X_1/v_1+X_2/v_2$, where X_i is the total distance the particle travels with velocity v_i. From these considerations we can conclude that the general form of the time-ordered and retarded Green's function for the case of isolated impurities is

$$\begin{aligned} g_{ij}(t,x,x')&=\sum_k L_k^{ij}\frac{1}{2\pi(T_k^{ij}-t+i\epsilon_t)},\\ g_{ij}^R(t,x,x')&=-i\theta(t)\sum_k L_k^{ij}\delta(T_k^{ij}-t), \end{aligned} \tag{168}$$

where the arrival times T_k^{ij} depend on the end points x and x' and the location of all impurities y_m located between the end points, and the coefficients L_k^{ij} depend on the impurity strengths q_m.

In calculating g_{ij} with N impurities between x' and x, these impurities divide the interval $[x',x]$ into $N+1$ segments. Since we are computing g_{ij}, the first segment must be associated with a factor of $g_{ii}^{(0)}$ and the last segment with a factor of $g_{jj}^{(0)}$. Since on the $N-1$ remaining segments we can have either $g_{11}^{(0)}$ or $g_{22}^{(0)}$ depending on the parity of the n_m, there are in general 2^{N-1} arrival times T_k^{ij}, and thus the number of terms in the sum in Eq. (168) grows exponentially with the number of intervening impurities.

For a given arrival time T_k^{ij}, the parities of the n_m's are determined and the corresponding coefficient L_k^{ij} in Eq. (168) is given by

$$L_k^{ij}=c_{ij}\prod_{m=1}^{N} r_{m,p_m}, \tag{169}$$

where $c_{ii}\equiv 1/v_i$, $c_{12}\equiv i/\sqrt{v_1v_2}\equiv -c_{21}$ are overall coefficients, $p_m=n_m \bmod 2$ is the parity of n_m, and

$$\begin{aligned} r_{m,0}&\equiv\sum_{n=0}^{\infty}\left(\frac{iq_m}{\sqrt{v_1v_2}}\right)^{2n}=\frac{1}{1+q_m^2/v_1v_2},\\ r_{m,1}&\equiv\sum_{n=0}^{\infty}\left(\frac{iq_m}{\sqrt{v_1v_2}}\right)^{2n+1}=\frac{iq_m/\sqrt{v_1v_2}}{1+q_m^2/v_1v_2}, \end{aligned} \tag{170}$$

where we have assumed $|q_m^2/v_1v_2|<1$ for all m. The coefficient $r_{m,0(1)}$ is the sum of the amplitudes for scattering off the mth impurity an even (odd) number of times.

For a given realization of the potential in Eq. (167), the Green's functions in Eq. (168), considered as functions of time, have an exponentially large number of singularities. However, the disorder-averaged quantities, $\overline{g}$ (128) and $\overline{g^R}$ [Eq. (150)], are very simple functions of time. This is readily understood if we approximate the white-noise potential by taking the impurity strengths q_m in Eq. (167) to be independent, identically distributed random variables with zero means. Then from Eq. (170) we see $\overline{r_{m,1}}=0$ for all m. Thus the only nonvanishing L_k^{ij} involves an even number of scatterings off each impurity, and hence there is only *one* singularity, corresponding to the particle never changing its velocity:

$$\overline{g_{ij}}(t,x,0)=\delta_{ij}\frac{1}{2\pi(x-x'-v_jt+i\epsilon_t)}(\overline{r_{m,0}})^N. \tag{171}$$

From Eq. (170) we see that $\overline{r_{m,0}}<1$, and since N, the number of impurities between x' and x, is proportional to $|x-x'|$, the last factor in Eq. (171) reproduces the exponential decay present in Eq. (128).

We can understand several things from the general form of the Green's functions given in Eq. (168). First note that the fact that g^R for the case of isolated δ-function impurities is a sum of δ functions in time [Eq. (168)] is consistent with the $\delta(t-t')$ factor present in $\overline{g_{ij}^R(t,x,0)g_{ij}^{R*}(t',x,0)}$ [Eq. (152)]. One can similarly show that the form of g in Eq. (168) is consistent with the $1/(t-t')$ behavior of $\overline{g_{ij}(t,x,0)g_{ij}^*(t',x,0)}$ [Eq. (151)].

Next we suppose that the N impurities between x' and x are evenly spaced. In the limit $N\to\infty$ it should not make a difference. In this case, Eq. (168) still holds but the quantities L_k^{ij} and T_k^{ij} are determined by a different set of rules, so we shall distinguish them by a tilde. The number of arrival times $\tilde{T}_k^{ij}$ is reduced from 2^{N-1} down to N. This is because the interval $|x'-x|$ is now divided into $N+1$ segments of *equal* length. The velocity on the first and last segments is fixed by the indices on g_{ij} and the N arrival times can then be specified by the number k of the $N-1$ remaining segments that have velocity v_2. For example, for g_{11} the arrival times are

$$\tilde{T}_k^{11}=\left(\frac{k}{v_2}+\frac{N+1-k}{v_1}\right)\frac{|x-x'|}{N+1}, \tag{172}$$

where $k=0,1,\ldots,N-1$. The amplitude $\tilde{L}_k^{ij}$ is the sum of $\binom{N-1}{k}$ of the L_k^{ij}'s given in Eq. (169). In the limit of large N the number of terms that contribute to $\tilde{L}_k^{ij}$ is a Gaussian distribution in k peaked at $k=(N-1)/2$. The arrival time corresponding to this amplitude is

$$\tilde{T}^{11}_{(N-1)/2}=\left(\frac{N-1}{2v_2}+\frac{N+3}{2v_1}\right)\frac{|x-x'|}{N+1}$$

$$\overset{N\to\infty}{\to} \frac{v_n|x-x'|}{v_1v_2}=t_0. \tag{173}$$

Thus we find that the mean arrival time t_0 emerges in this model potential because the number of terms that contribute to the singularity at $\tilde{T}_k^{ij}$ is maximal for $\tilde{T}_k^{ij}=t_0$.

All of the considerations in this section lead us to the conclusion that $D^R(t,x,x')$ in a typical configuration is given by $\overline{D^R}(t,x,x')$, Eq. (146), with the factor of $\mathrm{P}[1/(t_0-t)]$ replaced by a function $f(t,x,x')$, which is a rapidly fluctuating function of time, antisymmetric about the point $t=t_0$, and whose amplitude grows as t approaches t_0. The claim that the general structure of D^R in a typical configuration is captured by $\overline{D^R}$ is supported by the relation between D^R and g,g^R [Eq. (149)], and the fact that the second moments $\overline{|g|^2}$ and $\overline{|g^R|^2}$ [Eq. (152)] have the same structure as $\overline{D^R}$, without the principal value factor. We expect that $f(t,x,x')$ is a rapidly fluctuating function of time based on the dependence of $\overline{g_{ij}(t,x,0)g_{ij}^*(t',x,0)}$ and $\overline{g_{ij}^R(t,x,0)g_{ij}^{R*}(t',x,0)}$ on $(t-t')$, Eqs. (151) and (152), and the behavior of g and g^R for the case of isolated δ-function impurities, Eq. (168). However complicated $f(t,x,x')$ is, we know it must be antisymmetric about $t=t_0$ by Eq. (164). The claim that the amplitude of $f(t,x,x')$ approaches a maximum at $t=t_0$ is supported by several results. First, recall that g^R in a constant potential Γ, Eq. (166), is oscillatory with a frequency that is proportional to Γ and that is minimal at the mean arrival time. This suggests that in a potential that varies with x there will be less cancellation near the mean arrival time than near the extremal arrival times. Second, there is the observation that in the model of equally spaced isolated impurities the number of terms that contribute to each singularity is maximal for the singularity at the mean arrival time. Finally, we have the fact that averaging produces a function that is singular at $t=t_0$. These conclusions are supported by our numerical simulations; see Sec. II.

D. Pfaffian edge

In this section we consider the edge theory of the Pfaffian state, concentrating on the form of the retarded density response function in the presence of a finite temperature and disorder. The edge theory of the Pfaffian state contains a $c=1/2$ minimal model conformal field theory (CFT) in addition to the usual $(c=1)$ chiral boson.[18] Recall that the $c=1/2$ minimal model has three primary fields, which we denote as I, χ, and σ, and whose scaling dimensions are 0, 1/2, and 1/16, respectively. The χ field is identical to a single chiral Majorana fermion. The chiral boson in the edge theory, φ, can be shown to have a compactification radius of $R=1/\sqrt{8}$, the same radius as the charged mode of the 331 state; see I. In addition to the $c=1/2$ primary fields and their descendents, the operator content of the edge theory includes the primary field $\partial_x\varphi$ and the vertex operators $e^{ik\varphi/\sqrt{8}}$, where $k\in\mathbb{Z}$. The electron creation operator is[24]

$$:\Psi^\dagger(x):=\frac{1}{2\pi a}\chi(x)e^{-i\sqrt{2}\varphi(x)}, \tag{174}$$

which has a scaling dimension of 3/2.

We now determine the electric charge density operator, $\rho(x)$, for the Pfaffian edge. One requirement for this operator is that the electron operator has a unit charge with respect to it:

$$[\rho(x),\Psi^\dagger(x')]=\delta(x-x')\Psi^\dagger(x'). \tag{175}$$

One candidate that satisfies this relation is

$$\rho(x)=\frac{1}{2\pi\sqrt{2}}\partial_x\varphi(x). \tag{176}$$

The operator on the r.h.s. of this equation has dimension one. The only other dimension-one operators present in the edge theory are $e^{\pm i\sqrt{2}\varphi}$. However, if we were to add to our definition of $\rho(x)$ some nonzero multiple of the Hermitian combination $(e^{i\sqrt{2}\varphi}+e^{-i\sqrt{2}\varphi})$, we would find that the condition (175) is violated. Any other higher-dimension operators that could be added to $\rho(x)$ would necessarily be multiplied by explicit powers of the short-distance cutoff a, and will therefore vanish in the continuum limit. The Pfaffian state has no interlayer dynamics. Each electron is in a state symmetric between the layers, under the assumption that the symmetric-antisymmetric splitting is large. Hence, there is an energy gap for any process that excites the layers independently.

Having determined the charge density operator for the Pfaffian edge theory, we can immediately write down the retarded density two-point correlation function at zero temperature for the clean system:

$$\mathcal{D}^R_{\mathrm{Pf}}(t,x)=-\frac{1}{4\pi}\theta(t)\delta'(x-v_\varphi t). \tag{177}$$

From the results in Sec. III C we know that the only RG nonirrelevant disorder is scalar potential disorder. This does not modify $\mathcal{D}^R_{\mathrm{Pf}}$ at all, just as in the case of the charged mode for both the 110 and 331 sequences. From the discussion in Sec. II D we know that at a finite temperature this correlation function is also unchanged. We find that $\mathcal{D}^R_{\mathrm{Pf}}(t,x)$ has a signal at a single velocity even at a finite temperature and in the presence of a nonzero scalar potential.

E. Numerics

Here we briefly discuss the numerics for the neutral-mode contribution to the retarded density response function of the 331 edge. The matrices $S(x,0;\omega)$ were computed using a discretized version of Eq. (154). Using Eq. (153) the single-

particle Green's function was then found by a fast Fourier transform (FFT) algorithm. Finally, we used the relation between the single-particle Green's functions and the density response function (148) to calculate D^R, and integrated over time to find the neutral-mode contribution to the signal in Eq. (29).

ACKNOWLEDGMENTS

We would like to thank A. H. MacDonald for suggesting we consider gated samples, and C. de C. Chamon for bringing Ref. 13 to our attention. We would like to acknowledge support by the NSF (J.D.N.), DOE Grant No. DE-FG02-90ER40542 (L.P.P.) as well as NSF grant No. DMR-99-78074, US-Israel BSF grant No. 9600294, and support from the A. P. Sloan Foundation and the David and Lucille Packard Foundation (S.L.S.). L.P.P. and S.L.S. thank the Aspen Center for Physics for its hospitality during the completion of part of this work.

APPENDIX A: DISORDERED 331 SEQUENCE VIA THE SPIN ANALOGY

In this appendix we present an alternative method for obtaining exact disorder-averaged correlation functions for the 331 sequence. It is similar to the method used in our discussion of the 110 sequence in Sec. III C, with some technical complications. The procedure is based on the fact that we can explicitly construct solutions to the Heisenberg equations of motion for each realization of disorder. We shall ignore the charged mode throughout the discussion.

The 331 Hamiltonian including a disordered scalar potential (123) expressed in terms of the Dirac field is

$$\mathcal{H}_D=\int_{-L/2}^{L/2}dx:\Big[-iv_{\rm n}\psi^\dagger\partial_x\psi-i\frac{\lambda}{2\pi}(\psi^\dagger\partial_x\psi^\dagger+\psi\partial_x\psi)+\xi(x)\psi^\dagger\psi\Big]:, \tag{A1}$$

where in this appendix we suppress the subscript on ξ and take periodic boundary conditions $\psi(x+L)=\psi(x)$. The Heisenberg equations of motion for the field operator $\psi(t,x)$ and its Hermitian conjugate are

$$\begin{aligned}[\partial_t+v_{\rm n}\partial_x+i\xi(x)]\psi(t,x)+(\lambda/\pi)\partial_x\psi^\dagger(t,x)=0,\\ [\partial_t+v_{\rm n}\partial_x-i\xi(x)]\psi^\dagger(t,x)+(\lambda/\pi)\partial_x\psi(t,x)=0.\end{aligned} \tag{A2}$$

The anomalous (i.e., fermion-number nonconserving) terms in $\mathcal{H}_D$ couple the equations of motion for ψ and $\psi^\dagger$ and therefore we must expand the field in terms of both creation and annihilation operators,

$$\psi(t,x)=\sum_n\,[A_n(x)e^{-i\omega_n t}a_n+B_n(x)e^{i\omega_n t}a_n^\dagger], \tag{A3}$$

where by assumption $a_n^\dagger$ are canonical Fermi operators that create exact single-particle eigenstates of $\mathcal{H}_D$ with energies ω_n. Substituting this expansion into the equations of motion leads to the following matrix differential equation:

$$-iQ\partial_x f_n(x)=[\omega_n\mathbb{1}-\xi(x)\sigma^z]f_n(x), \tag{A4}$$

where

$$Q\equiv\begin{pmatrix}v_{\rm n}&\lambda/\pi\\ \lambda/\pi&v_{\rm n}\end{pmatrix},\quad f_n(x)\equiv\begin{pmatrix}A_n(x)\\ B_n^*(x)\end{pmatrix}. \tag{A5}$$

Note that the Hamiltonian (A1) has a particle-hole symmetry under which $\psi\leftrightarrow\psi^\dagger$ and $\xi\mapsto-\xi$. In terms of the two-component wave function $f_n(x)$, this implies that if f_n is a solution to Eq. (A4) with energy ω_n, then $\tilde f_n=\sigma^x f_n^*$ is a solution with energy $-\omega_n$. Assuming all $\omega_n\neq0$, we can enumerate the functions $f_n(x)$ in such a way that $\omega_{-n}=-\omega_n$ and $\omega_n>0$ for $n>0$. This implies $\tilde f_{-n}=f_n$, from which we find $A_n=B_{-n}$, an indication that some double counting may be present. Indeed, the particle-hole symmetry only interchanges the two equations (A2); it should not generate new solutions. This double counting can be removed if we define $a_n+a_{-n}^\dagger\mapsto a_n$, and write, instead of Eq. (A3),

$$\begin{pmatrix}\psi(t,x)\\ \psi^\dagger(t,x)\end{pmatrix}=\sum_n\,f_n(x)\,e^{-i\omega_n t}a_n. \tag{A6}$$

To obtain the solutions to Eq. (A4) we define the rescaled wave functions

$$\zeta_n=Q^{1/2}f_n, \tag{A7}$$

in terms of which the differential equation (A4) becomes

$$\partial_x\zeta_n(x)=i\left[\omega_nQ^{-1}-\frac{\xi(x)}{\sqrt{v_1v_2}}\sigma^z\right]\zeta_n(x). \tag{A8}$$

We can write the solutions to this equation as

$$\zeta_n(x)\equiv S(x,0;\omega_n)\zeta_n(0), \tag{A9}$$

with a coordinate-ordered exponential

$$S(x,x';\omega)=T_y\exp\left(i\int_{x'}^{x}dy\left[\omega Q^{-1}-\frac{\xi(y)}{\sqrt{v_1v_2}}\sigma^z\right]\right), \tag{A10}$$

for $x>x'$, and the Hermitian conjugate $S(x,x';\omega)=S^\dagger(x',x;\omega)$ for $x<x'$. The boundary conditions on the Fermi field imply $\zeta_n(x+L)=\zeta_n(x)$, which in turn means that the allowed energies ω_n are determined by finding those energies for which the matrix $S(L,0;\omega)$ has a unit eigenvalue with the corresponding eigenvector taken to be $\zeta_n(0)$,

$$[S(L,0;\omega)-\mathbf{1}]\zeta_n(0)=0. \tag{A11}$$

The orthogonality of solutions $f_n(x)$ for different values of ω_n is guaranteed by the fact that the differential equation (A4) is self-conjugate, while their normalization must be demanded explicitly,

$$\int_{-L/2}^{L/2}dx\,f_n^\dagger(x)f_n(x)=1. \tag{A12}$$

This can be rewritten with the help of Eqs. (A7) and (A9) as

$$L\frac{v_n}{v_1 v_2}\zeta^\dagger(0)\mathcal{N}(\omega,\xi)\zeta(0)=1,$$
$$\mathcal{N}(\omega,\xi)=\mathbb{1}-\frac{\lambda}{\pi v_n L}\int_{-L/2}^{L/2}dx\, S^\dagger(x,0;\omega)\sigma^x S(x,0;\omega). \tag{A13}$$

Usually it is the wave-function normalization that makes the disorder calculations so difficult. Note, however, that the integration in the second term of the normalization matrix $\mathcal{N}(\omega,\xi)$ is extended over the entire length of the sample, which makes it a self-averaging object. As in Sec. III C, the matrix $S(x,x';\omega)$ [Eq. (A10)] can be interpreted as the evolution operator in a fictitious time y, for a spin precessing under the influence of a constant magnetic field in the x direction (due to the off-diagonal terms of the matrix Q^{-1}), and a random field $\sim\xi(x)$ along the z direction. The integral in Eq. (A13) is the x component of the spin averaged over a ''time'' L. In the presence of a nonvanishing disorder, the initial orientation is forgotten after a finite distance, and the second term in the normalization matrix (A13) disappears in the thermodynamic limit, $L\to\infty$. This happens with probability 1 for any realization of disorder. Physically, this simplification is related to the fact that in a chiral system localization does not happen; each particle explores the entire circumference of the sample.

Let us now consider the single-particle Green's function of the neutral-mode fermion, $\mathcal{G}_\psi$ [Eq. (71)]. Using Eq. (A6), this can be written

$$\mathcal{G}_\psi(t,x,x')=-i\sum_n f_n(x)f_n^\dagger(x')e^{-i\omega_n t}[\theta(t)\,n(-\omega_n) - \theta(-t)\,n(\omega_n)], \tag{A14}$$

where $n(\omega)\equiv[\exp(\beta\omega)+1]^{-1}$ is the usual Fermi distribution function. Using Eqs. (A7), (A9), and (A13), with $\mathcal{N}(\omega,\xi)=\mathbb{1}$, we obtain

$$\mathcal{G}_\psi(t,x,x')=-i\left(\frac{v_1v_2}{Lv_n}\right)\sum_n e^{-i\omega_n t}[\theta(t)n(-\omega_n)-\theta(-t)n(\omega_n)]Q^{-1/2}\left[S(x,0,\omega_n)\frac{\zeta_n(0)\zeta_n^\dagger(0)}{\zeta_n^\dagger(0)\zeta_n(0)}S^\dagger(x',0,\omega_n)\right]Q^{-1/2}, \tag{A15}$$

where $\zeta_n(0)$ obey the eigenvalue equation (A11). To take the thermodynamic limit, we need to set the system size to infinity, keeping other parameters (temperature, disorder, distance $|x-x'|$, etc.) finite. Effectively, this implies that we can select an energy interval ΔE, ''infinitesimal'' on a scale defined by these finite quantities, and yet containing a macroscopic number of energy levels, such that the averaging over the states within this interval gives

$$\langle\zeta_n\zeta_n^\dagger\rangle_{\omega_n\in\Delta E}=\frac{1}{2}\mathbf{1}.$$

The value of the average and the existence of such an interval follows from the fact that for any $\omega_1\neq\omega_2$, the spin-rotation matrices $S(L,0;\omega_{1,2})$ become entirely uncorrelated for a sufficiently large L, or, equivalently, the relative rotation matrix $S^\dagger(L,0;\omega_1)S(L,0;\omega_2)$ entirely forgets the initial direction.

Performing the averaging over the eigenstates within such an interval, we obtain for the correlation function (A15),

$$\mathcal{G}_\psi(t,x,x')=-i\int\frac{d\omega}{2\pi}e^{-i\omega t}[\theta(t)n(-\omega) - \theta(-t)n(\omega)]Q^{-1/2}S(x,x';\omega)Q^{-1/2}, \tag{A16}$$

where the summation was replaced by an integration using the ''clean'' single-particle total density of states $\overline{\rho}=(v_1^{-1}+v_2^{-1})L=2Lv_n/v_1v_2$, which cannot be modified by disorder. Note that Eq. (A16) does not contain a disorder average; it is an expression valid for any given realization of disorder (or even in the limit of no disorder, as long as this limit is taken *after* the thermodynamic limit). For example, we checked that Eq. (A16) with $\xi(x)=\text{const}$ reproduces Eq. (74), which was derived by more conventional methods.

From the definition of $S(x,x';\omega)$, Eq. (A10), and the disorder-averaging procedure used previously, see Eq. (113), we find

$$\overline{S(x,x';\omega)}=e^{-\Delta_\xi|x-x'|/2v_1v_2}e^{i\omega(x-x')Q^{-1}}. \tag{A17}$$

With the help of Eqs. (70) and (A16) this gives, in the zero-temperature limit,

$$\overline{\mathcal{G}(t,x,0)}\equiv\frac{1}{[2\pi(x-v_c t+i\epsilon_t)]^{m-1}}\frac{1}{2}\left[\frac{\mathbb{1}+\sigma^x}{2\pi(x-v_1t+i\epsilon_t)} + \frac{\mathbb{1}-\sigma^x}{2\pi(x-v_2t+i\epsilon_t)}\right]e^{-\Delta_\xi|x|/2v_1v_2}. \tag{A18}$$

This is in exact agreement with Eq. (130) of Sec. III C. We have checked that the other disorder-averaged correlation functions for the 331 sequence discussed in Sec. III C can also be reproduced using the method described in this appendix.

APPENDIX B: RANDOM TUNNELING FOR THE 331 SEQUENCE

In this appendix we illustrate the effect of an RG irrelevant random perturbation by analyzing the neutral mode of the 331 bilayer in the presence of velocity and tunneling

disorder. Specifically, we assume that both the neutral-mode velocity $v_n(x)$ and the tunneling amplitude $\lambda(x)$ in Eq. (A1) are coordinate-dependent, in such a fashion that the system remains chiral, $v_{1,2}(x)=v_n(x)\pm\lambda(x)/\pi>0$ for all x. The introduction of such a coordinate dependence requires only a slight modification of the Hamiltonian (A1). Specifically, the first term in the Hamiltonian density must be replaced as

$$-iv_n\psi^\dagger\partial_x\psi\rightarrow-\frac{i}{2}\{v_n(x)\psi^\dagger\partial_x\psi+\psi^\dagger\partial_x[v_n(x)\psi]\}.$$

The arguments in Appendix A can then be repeated with little modification and we obtain, in place of Eqs. (A15) and (A10),

$$\mathcal{G}_\psi(t,x,x')=\int\frac{d\omega}{2\pi i}e^{-i\omega t}[\theta(t)n(-\omega)-\theta(-t)n(\omega)]Q^{-1/2}(x)S(x,x';\omega)Q^{-1/2}(x'),\tag{B1}$$

$$S(x,x';\omega)=T_y\exp\left(i\int_{x'}^{x}dy[\omega Q^{-1}(y)-u(y)\sigma_z]\right),$$

$$u(y)\equiv\frac{\xi(y)}{v_1^{1/2}(y)v_2^{1/2}(y)}.\tag{B2}$$

Again, this expression is valid for any given configuration of disordered $v_n(x)$, $\lambda(x)$, and $\xi(x)$.

The requirement $v_{1,2}(x)>0$ is equivalent to essentially non-Gaussian disorder, and the disorder averaging is generally nontrivial. This, however, is greatly simplified in the absence of potential disorder, $\xi(x)=0$. In this case the remaining matrices $Q^{-1}(y)$ in the exponential commute with one another for all y, the coordinate ordering (T_y) can be omitted, and the disorder averaging can be performed directly. The structure of the expression is most evident after the unitary transformation (129) to the Majorana fermion representation,

$$g_{ij}(t,x,x')=O^\dagger\mathcal{G}_\psi(t,x,x')O=\int\frac{d\omega}{2\pi i}e^{-i\omega t}[\theta(t)n(-\omega)-\theta(-t)n(\omega)]\frac{\delta_{ij}\exp[i\omega\tau_i(x,x')]}{v_i^{1/2}(x)v_i^{1/2}(x')},\tag{B3}$$

where $\tau_i(x,x')\equiv\int_{x'}^{x}dy/v_i(y)$ is the time it takes for the ith mode to travel from x' to x. Clearly, the structure of the correlation function in a given configuration of disorder does not change; at zero temperature we obtain [cf. Eqs. (6) and (130)]

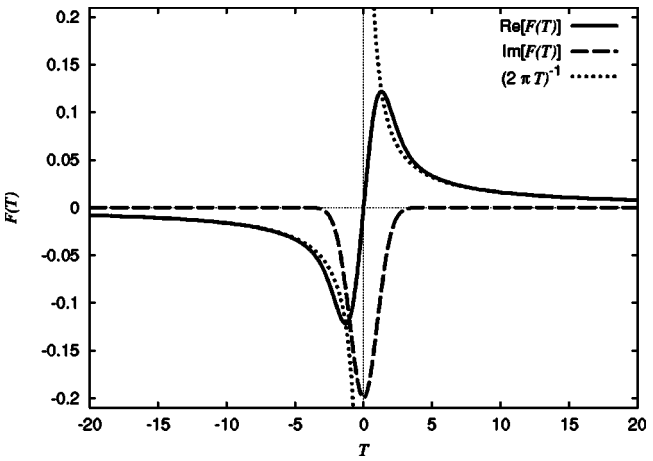

FIG. 13. The real (solid line) and imaginary (dashed line) parts of the universal function $F(T)$ [Eq. (B4)], which describes the shape of the peaks of the averaged Green's function for the 331 double layer with disorder in the tunneling amplitude. The dotted line shows the real part of the Green's function in the absence of disorder.

$$\mathcal{G}_\psi(t,x,x')=\frac{1}{4\pi}\left[\frac{\mathbb{1}+\sigma^x}{v_1^{1/2}(x)v_1^{1/2}(x')[\tau_1(x,x')-t]}+\frac{\mathbb{1}-\sigma^x}{v_2^{1/2}(x)v_2^{1/2}(x')[\tau_2(x,x')-t]}\right].$$

The disorder averaging can be performed for weak disorder if we notice that the velocity fluctuations along the entire path contribute to the arrival times $\tau_i(x,x')$; these quantities acquire nearly Gaussian distributions at sufficiently large distances (compared to the disorder correlation length, $l_c\ll|x-x'|$). If we ignore small multiplicative corrections near the ends of the interval, we then find

$$\overline{\mathcal{G}_\psi(t,x,0)}=\frac{1}{4\pi}\left[(\overline{v_1^{-1/2}})^2\frac{\mathbb{1}+\sigma^x}{D_1^{1/2}}F(T_1/D_1^{1/2})+(\overline{v_2^{-1/2}})^2\frac{\mathbb{1}-\sigma^x}{D_2^{1/2}}F(T_2/D_2^{1/2})\right],$$

where $T_i=T_i(x)\equiv\overline{\tau_i}(x)-t$ is the time elapsed from the arrival of the ith peak, $D_i=D_i(x)\equiv\overline{\tau^2}(x)-\overline{\tau}^2(x)$ is the corresponding dispersion, and

$$F(T)\equiv\int_0^\infty\frac{d\omega}{2\pi i}e^{i\omega T-\omega^2/2},\tag{B4}$$

where we have assumed $t>0$. As illustrated in Fig. 13, at large values of the argument, this function approaches asymptotically the clean single-particle Green's function, $F(T)=(2\pi T)^{-1}$, $|T|\gg1$. Although the perturbation is RG irrelevant, the form of the Green's function is modified in the vicinity of the singularities.

For a weak ($w\ll v_n$) Gaussian disorder with a finite correlation length,

$$\lambda(x)=\overline{\lambda}+\delta\lambda(x), \quad \langle \delta\lambda(x)\,\delta\lambda(y)\rangle = w^2 f(x-y),$$

$$f(0)=1,$$

assuming $w^2 \ll \overline{\lambda}^2$, we obtain, to leading order in the weak disorder expansion,

$$\overline{\tau_i(x)} = (x/\overline{v})[1+w^2/\pi^2\overline{v_i}^2 + O(w^4/\overline{v_i}^4)],$$

and $D_i(x)=w^2 x l_c/v_i^4+\cdots$, where the disorder correlation length

$$l_c=\int_0^\infty dx\, f(x)$$

was assumed to be short compared with the overall distance, $l_c \ll |x|$.

APPENDIX C: EVALUATION OF INTEGRALS

In this appendix we evaluate the integrals needed in the main text. The basic integral is of the form

$$A(\tau,X)=\int_{-\infty}^{\infty}\frac{d\omega}{2\pi}e^{i\omega\tau}\frac{\sinh[\Lambda(\omega)X]}{\Lambda(\omega)}, \tag{C1}$$

where $\Lambda(\omega)=\sqrt{a^2-b^2\omega^2}$, and τ, X, a, and b are real parameters. At large frequencies the integrand is of the form $1/\omega$ times an oscillatory function and therefore converges without a regulator. Also, since the expansion of the integrand in powers of $\Lambda(\omega)$ contains only even powers, no branch cut is needed and the integrand is therefore an analytic function for finite ω. For large ω the integrand contains the factors $e^{i\omega(\tau\pm bX)}$. Thus for $|bX|<|\tau|$, the integrand is exponentially small on one side of the real axis and we can therefore close the contour on that side and find $A=0$; hence

$$A(\tau,X)\propto\theta((bX)^2-\tau^2). \tag{C2}$$

To evaluate the integral in the region for which it is nonzero, we break up the integral into two terms:

$$A(\tau,X)=\int_{C_1}\frac{d\omega}{2\pi}e^{i\omega\tau}\frac{e^{\Lambda(\omega)X}}{2\Lambda(\omega)}-\int_{C_2}\frac{d\omega}{2\pi}e^{i\omega\tau}\frac{e^{-\Lambda(\omega)X}}{2\Lambda(\omega)}, \tag{C3}$$

where now we must introduce a branch cut, which we take to run along the real ω axis from $-a/b$ to a/b. The contours C_1 and C_2 are shown in Fig. 14. Assuming $X>0$, the contours have been chosen so that the integrals in Eq. (C3) are separately convergent. The integrand in the C_2 integral is exponentially small in the upper half-plane and thus can be closed there to give zero. The integrand in the C_1 integral is exponentially small in the lower half-plane and can be closed there and contracted to run around the branch cut. We use the change of variables $\omega=(a/b)\sin\varphi$ in the integral around the cut to arrive at

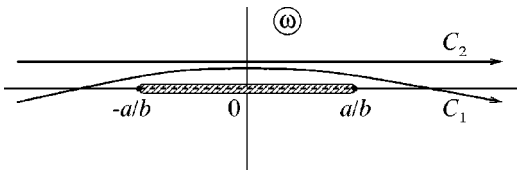

FIG. 14. The complex ω plane showing the branch cut along the real ω axis and the contours C_1 and C_2.

$$A(\tau,X)=\theta((bX)^2-\tau^2)\frac{1}{2b}\int_0^{2\pi}\frac{d\varphi}{2\pi}e^{a[i(\tau/b)\sin\varphi+X\cos\varphi]}. \tag{C4}$$

We next note that we can write

$$i\frac{\tau}{b}\sin\varphi+X\cos\varphi=\sqrt{X^2-\left(\frac{\tau}{b}\right)^2}\cos(\varphi-i\varphi_0), \tag{C5}$$

where the real parameter φ_0 is defined by $\cosh\varphi_0=X/\sqrt{X^2-(\tau/b)^2}$. After performing this substitution in Eq. (C4) and noting that the integrand is a periodic function in φ with period 2π, we can perform a final change of variables $\theta=\varphi-i\varphi_0$ to find

$$A(\tau,X)=\theta((bX)^2-\tau^2)\frac{1}{2b}\int_0^{2\pi}\frac{d\theta}{2\pi}e^{a\sqrt{X^2-(\tau/b)^2}\cos\theta}$$

$$=\frac{1}{2b}\theta[(bX)^2-\tau^2]I_0\left(\frac{a}{b}\sqrt{(bX)^2-\tau^2}\right), \tag{C6}$$

where I_0 is a Bessel function of imaginary argument.

Using $a=\Delta_\xi$, $b=\lambda/\pi$, $\tau=v_n X-t$ and differentiating Eq. (C6) with respect to τ and X give the following results:

$$\int_{-\infty}^{\infty}\frac{d\omega}{2\pi}e^{i\omega(v_n X-t)}\frac{\sinh[\Lambda(\omega)X]}{\Lambda(\omega)}$$

$$=\frac{1}{2(\lambda/\pi)}\theta(z)I_0\left(\frac{\Delta_\xi}{\lambda/\pi}\sqrt{z}\right), \tag{C7}$$

$$\int_{-\infty}^{\infty}\frac{d\omega}{2\pi}e^{i\omega(v_n X-t)}\cosh[\Lambda(\omega)X]=\frac{1}{2}\,\mathrm{sgn}(t)[\,\delta(x/v_1-t)+\delta(x/v_2-t)] \quad +\frac{\Delta_\xi}{2v_1v_2}\theta(z)\frac{x}{\sqrt{z}}I_1\left(\frac{\Delta_\xi}{\lambda/\pi}\sqrt{z}\right), \tag{C8}$$

$$\int_{-\infty}^{\infty}\frac{d\omega}{2\pi}e^{i\omega(v_n X-t)}i\omega\frac{\sinh[\Lambda(\omega)X]}{\Lambda(\omega)}=-\frac{1}{2\lambda/\pi}\,\mathrm{sgn}(t)[\,\delta(x/v_1-t)-\delta(x/v_2-t)]-\frac{\Delta_\xi}{2(\lambda/\pi)^2}\theta(z)\frac{(v_n x/v_1v_2-t)}{\sqrt{z}}I_1\left(\frac{\Delta_\xi}{\lambda/\pi}\sqrt{z}\right), \tag{C9}$$

where $z \equiv (t - x/v_1)(x/v_2 - t)$.

Finally, if we analytically continue the above results to the case of $\Delta_\xi = i\sqrt{v_1 v_2}\Gamma$, where Γ is real, and write $\kappa(\omega) = \sqrt{v_1 v_2 \Gamma^2 + (\lambda/\pi)^2 \omega^2}$, we find

$$\int_{-\infty}^{\infty} \frac{d\omega}{2\pi} e^{i\omega(v_n X - t)} \frac{\sin[\kappa(\omega)X]}{\kappa(\omega)} = \frac{1}{2(\lambda/\pi)} \theta(z) J_0\left(\frac{\Gamma}{\lambda/\pi}\sqrt{v_1 v_2 z}\right), \tag{C10}$$

$$\int_{-\infty}^{\infty} \frac{d\omega}{2\pi} e^{i\omega(v_n X - t)} \cos[\kappa(\omega)X] = \frac{1}{2}\,\mathrm{sgn}(t)[\delta(x/v_1 - t) + \delta(x/v_2 - t)] - \frac{\Gamma}{2}\theta(z)\frac{x}{\sqrt{v_1 v_2 z}} J_1\left(\frac{\Gamma}{\lambda/\pi}\sqrt{v_1 v_2 z}\right), \tag{C11}$$

$$\int_{-\infty}^{\infty} \frac{d\omega}{2\pi} e^{i\omega(v_n X - t)} i\omega \frac{\sin[\kappa(\omega)X]}{\kappa(\omega)} = -\frac{1}{2\lambda/\pi}\,\mathrm{sgn}(t)[\delta(x/v_1 - t) - \delta(x/v_2 - t)] + \frac{\Gamma\theta(z)}{2(\lambda/\pi)^2}\frac{(v_n x - v_1 v_2 t)}{\sqrt{v_1 v_2 z}} J_1\left(\frac{\Gamma\sqrt{v_1 v_2 z}}{\lambda/\pi}\right). \tag{C12}$$

---

*Present address: Department of Physics, University of California, Riverside, CA, 92521.

[1] B.I. Halperin, Phys. Rev. B **25**, 2185 (1982).

[2] X.-G. Wen, Phys. Rev. B **41**, 12 838 (1990).

[3] C.L. Kane and M.P.A. Fisher, in *Novel Quantum Liquids in Low-Dimensional Semiconductor Structures*, edited by S. DasSarma and A. Pinczuk (Wiley, New York, 1995).

[4] E. Witten, Commun. Math. Phys. **121**, 351 (1989).

[5] G. Moore and N. Read, Nucl. Phys. B **360**, 362 (1991).

[6] A.M. Chang, L.N. Pfeiffer, and K.W. West, Phys. Rev. Lett. **77**, 2538 (1996).

[7] M. Grayson, D.C. Tsui, L.N. Pfeiffer, K.W. West, and A.M. Chang, Phys. Rev. Lett. **80**, 1062 (1998).

[8] N. Read and E. Rezayi, Phys. Rev. B **59**, 8084 (1999).

[9] J.D. Naud, L.P. Pryadko, and S.L. Sondhi, Nucl. Phys. B **565**, 572 (2000).

[10] If one includes the possibility of constrictions one can also probe the dimensions of quasiparticle operators.

[11] K. Ino, Phys. Rev. Lett. **81**, 1078 (1998).

[12] L.S. Levitov, A.V. Shytov, and B.I. Halperin, cond-mat/0005016 (unpublished).

[13] X.-G. Wen, Phys. Rev. B **50**, 5420 (1994).

[14] C.L. Kane, M.P.A. Fisher, and J. Polchinski, Phys. Rev. Lett. **72**, 4129 (1994).

[15] J.T. Chalker and S.L. Sondhi, Phys. Rev. B **59**, 4999 (1999).

[16] J. Eisenstein, in *Novel Quantum Liquids in Low-Dimensional Semiconductor Structures*, edited by S. DasSarma and A. Pinczuk (Wiley, New York, 1995).

[17] M. Greiter, X.-G. Wen, and F. Wilczek, Phys. Rev. Lett. **66**, 3205 (1991).

[18] K. Imura and K. Ino, Solid State Commun. **107**, 497 (1998).

[19] R.C. Ashoori, H.L. Stormer, L.N. Pfeiffer, K.W. Baldwin, and K. West, Phys. Rev. B **45**, 3894 (1992).

[20] I.J. Maasilta and V.J. Goldman, Phys. Rev. B **55**, 4081 (1997); **57**, R4273 (1998).

[21] X.-G. Wen and A. Zee, Phys. Rev. B **46**, 2290 (1992).

[22] T. Giamarchi and H.J. Schulz, Phys. Rev. B **37**, 325 (1988).

[23] I.E. Dzyaloshinskii and A.I. Larkin, Zh. Éksp. Teor. Fiz. **65**, 411 (1973) [Sov. Phys. JETP **38**, 202 (1974)].

[24] M. Milovanović and N. Read, Phys. Rev. B **53**, 13 559 (1996).